Information-theoretic Characterization of MIMO Systems with Multiple Rayleigh Scattering

Information-theoretic Characterization of MIMO Systems with Multiple Rayleigh Scattering

G. Alfano, *Student Member, IEEE,* C.-F. Chiasserini, *Senior Member, IEEE,* A. Nordio, *Member, IEEE*, and S. Zhou

Abstract

We present an information-theoretic analysis of a point-to-point Multiple-Input-Multiple-Output (MIMO) link affected by Rayleigh fading and multiple scattering, under perfect channel state information at the receiver. Unlike previous work addressing this setting, we investigate the Random Coding Error Exponent, its associated cutoff rate and the Expurgated Error Exponent, and derive closed-form expressions for them. Moreover, leveraging the average mutual information expression presented in [1], we derive another important metric, namely, the sum rate, under linear receive processing and independent stream decoding. In particular, we characterize the performance of the Minimum Mean Squared Error receiver in closed form, and that of the Zero Forcing receiver by resorting to bounding techniques. The bulk of the work relies on results about finite-dimensional random matrix products, a number of which are novel and detailed in the Appendices. The analysis, validated through numerical results, highlights the severe degradation in the performance of linear receivers due to multi-fold scattering. It also unveils the performance trend of multiple scattering MIMO channels as a function of the number of antennas and the number of scattering stages.

G. Alfano is with the Department of Science and Applied Technology, Politecnico di Torino, 10129 Italy e-mail: d020860@polito.it

C.-F. Chiasserini is with Department of Electronics, Politecnico di Torino, 10129 Italy, and a Research Associate at CNR-IEIIT, e-mail: chiasserini@polito.it

A. Nordio is with Wireless Communications Systems Group, CNR-IEIIT, Torino, 10129 Italy, e-mail: alessandro.nordio@ieiit.cnr.it

S. Zhou is with college of computer and information, Hohai university, China, e-mail: siyuan.zhou@hhu.edu.cn

Manuscript received January, 2017; revised October, 2017. Part of this work was presented at IEEE ISWCS 2015 [39] and at WSA 2016 [40] conferences.

Index Terms

MIMO, Random matrix products, Multiple Rayleigh scattering, Error exponents, Linear receivers.

I. INTRODUCTION

The presence of multiple (or multi-fold) scattering on the radio channel has been confirmed by early measurement campaigns [2], and has henceforth been taken into account in Multiple-Input-Multiple-Output (MIMO) channel modeling (see, e.g., the pioneering work in [3]). These works take into account, from the practical and the theoretical point of view, the presence of isolated or clustered obstacles of considerable size compared to the signal wavelength. The scattering effects due to such obstacles are relevant with respect to common diffusion phenomena caused by the presence of randomly placed impurities in the radio channel. Impairments caused by these objects are referred to as keyholes or pinholes (see, e.g., [4]) when they are correlated, thus leading to a rank-deficiency of the MIMO channel matrix. They are instead termed as multi-keyhole [5] (or, more in general, double or multiple scattering phenomena) in the presence of multiple objects causing uncorrelated scattering events. For a preliminary analysis of such phenomena in early MIMO literature, the reader is referred to [6]. Importantly, in the more recent literature, multi-fold scattering is considered as a relevant impairment of the radio channel in the analysis of the link between a pico-base station and a user [7, and references therein]. Analytical understanding of multiple scattering models is also a milestone towards a fair comparison between small-cells and the recently proposed cell-less paradigm (see e.g. [8]).

The presence of successive clusters of dominant scatterers affecting a MIMO link can be modeled as a product of N random matrices. The size of such matrices may vary from matrix to matrix and coincides with the number of dominant scatterers per cluster [7, and references therein]. Correlation between spatially separated clusters, as well as between scattering objects belonging to the same cluster (see [9]), is typically neglected for the sake of simplicity. Even after such a strong simplification, finite-size analysis of multiple scattering MIMO channels was considered to be impractical till very recently, due to the lack of closed-form characterization of the spectrum of the product of an arbitrary number of independent random matrices of finite size. A noticeable exception is the case of $N = 2$, i.e., the so-called *double scattering channel* [6], [10], [11], the simplified version of which is referred to as Rayleigh-product channel [12, and references therein]. A very large number of studies (not cited here for the sake of brevity)

have appeared on this case since very early MIMO analysis. Additionally, asymptotic analysis of MIMO links, where the channel matrix is represented by a product of a finite number of large-sized random matrices[1], has been focusing only on relay-aided settings (see, e.g., [13], [14]).

Finite-size analysis for an arbitrary N has become possible in closed form only after the seminal work in [1]. Therein, Akemann *et al.* provide an explicit expression for the marginal singular value distribution of a matrix product of N independent rectangular matrix factors, each having independent, standard complex Gaussian entries. As an instance of application of such spectral statistics, [1] provides a closed-form expression for the mutual information conveyed by a MIMO multiple scattering channel [1, Formula (82)] when Channel State Information (CSI) is available at the receiver. Using the result in [1], Wei *et al.* [7] present the first exact analysis of the above system in the case of orthogonal space-time block coding, while an approximate analysis for an arbitrary number of matrix factors and in a more general scenario is given in [15].

Yet all the aforementioned works address mutual information only. This motivated us to extend the analysis to the error exponent, the channel cutoff rate, and the sum rate achievable by linear receivers – metrics that are of paramount relevance in wireless communications. Indeed, while ergodic mutual information represents the channel performance when information is encoded using an (ideally) infinite block length, error exponent and cutoff rate illustrate how the channel behaves with finite block length. Specifically, the error exponent expresses the trade-off between the average block-error probability (corresponding to the optimum code) and the required coding length at a prescribed rate below the channel capacity.

We first focus on the Random Coding Error Exponent (RCEE), proposed by Gallager [16] and based on uniformly random selection of the codewords. We provide closed-form expressions for both the RCEE and its associated cutoff rate, in the multiple-scattering scenario. We also derive a closed-form expression for a refined version of the RCEE, called Expurgated Error Exponent (EEE) [16], where bad codewords are expurgated in order to decrease the error probability. We remark that previous studies tackling MIMO channels [17]–[21] have derived results[2] tailored to specific fading assumptions only and without multi-fold scattering, either in closed form or

[1]Despite model similarities with multiple scattering channels, the study of this aspect is beyond the scope of our work.

[2]In [22], where first the problem was formulated, there is no final analytic expression for the error exponent.

resorting to saddle-point approximations. Our evaluation of RCEE and EEE, instead, specifically addresses multiple-scattering MIMO channels and, as customary in the literature, it is performed under the assumption of CSI availability at the receiver only. It is also worth noticing that, without CSI at either link ends, the unique available result on the error exponent in MIMO systems is for Rayleigh channels and has been derived in [23]. Furthermore, the closed-form expressions that we obtain for the cutoff rate allow us to extensively study the channel behavior and provide interesting insights on the interplay between spatial degrees of freedom (the number of available antennas at either link end), fading degrees of freedom (the number of significant scattering stages), channel coherence, and coding length. It is worth mentioning that a detailed analysis of a MIMO product channel, focused on Lyapunov exponents instead of RCEE, can be found in [24], where the authors analyze an infinite product of finite-sized Rayleigh scattering matrices.

We then study the sum-rate performance of linear receivers, which, in proper signal-to-noise (SNR) ranges, provide close-to-optimal performance with limited computational burden. Previous closed-form analysis of the Minimum Mean-Squared Error (MMSE) receiver has been carried out for Rayleigh/Rayleigh-product or uncorrelated Ricean fading [12], [25]. Zero-forcing (ZF) receive processing, instead, has been investigated by Matthaiou *et al.* in [26], [27], where the authors provide bounds to the sum rate in the presence of Rayleigh fading. The performance of ZF and MMSE receivers have been compared in [28] in terms of the single-branch signal-to-interference-plus-noise-ratio (SINR), with and without large-scale fading, lognormal distributed component. In our study, we adopt the strategy proposed in [25] for the MMSE sum-rate evaluation, particularizing it to the multiple-scattering channel, and obtain a closed-form result. Finally, drawing upon [26] and [28], we analyze the ZF case and derive an upper and a lower bound to its sum rate. Interestingly, we find that, in the presence of multiple scattering, sum-rate bounds result to be very loose, with respect to their tight behavior in Rayleigh and Rice fading.

In summary, our main contributions are as follows:

- We first characterize the multiple-scattering channel by deriving closed-form expressions for the RCEE, its associated cutoff rate, and EEE, under the assumption that CSI is available at the receiver only. We remark that our methodology is general and allows the derivation of the error exponent for a large class of fading distributions;
- We also provide a spectral analysis of multiple-scattering matrices by deriving the expressions for the minimum, maximum and generic unordered eigenvalue;

- We then analyse the performance of a communication system in the presence of multiple-scattering channel, when linear receivers are adopted. In particular, we obtain a closed-form expression of the sum rate achieved by the MMSE receiver, and a lower and an upper bound for the ZF receiver;
- We validate our analysis through numerical results, and show the poor suitability of linear receivers for multiple-scattering channels and the impact of the number of scattering clusters on the system performance.

At last, we mention that we do not address spatially correlated systems. The impact of spatial correlation on the average asymptotic capacity of double-scattering channels has been quantified as early as in [3], while the corresponding effect on the variance of the mutual information has been handled in [11]. Very recently, a relevant study [9] has appeared on multiple-cluster scattering with spatial correlation at the end of the link with the least number of antennas. This is the only case for which exact results are currently available.

The rest of the paper is organized as follows. Sections II and III introduce, respectively, the notation we use in our analysis and the channel model we assume. Section IV presents our results on the eigenvalue decomposition, the generalized variance and the spectral transforms of the product of random matrices. We then derive results on the error exponent and on the cutoff rate in Section V. The mutual information and the sum rate for the MMSE and the ZF receivers are analysed in Section VI. Whenever appropriate, analytical results are complemented with numerical results for validation purposes. Finally, we draw our conclusions in Section VII.

II. NOTATION

A. Vectors and matrices

Boldface uppercase and lowercase letters denote matrices and vectors, respectively. The identity matrix is indicated by $\mathbf{I}$. The determinant and the conjugate transpose of the generic matrix $\mathbf{M}$ are denoted by $|\mathbf{M}|$ and $\mathbf{M}^{\mathsf{H}}$, respectively, while the (i,j)-th element of $\mathbf{M}$ is indicated by $[\mathbf{M}]_{i,j}$. The Frobenius norm of $\mathbf{M}$ is denoted by $\|\mathbf{M}\|^2 = \mathsf{Tr}\{\mathbf{M}\mathbf{M}^{\mathsf{H}}\}$ where Tr is the matrix trace operator. The $n \times n$ matrix $\mathbf{M}$ is sometimes denoted as $\mathbf{M} = \{[\mathbf{M}]_{i,j}\}_{i,j=1,\ldots,n}$. For any $n \times n$ Hermitian matrix $\mathbf{M}$ with eigenvalues $m_1, \ldots, m_n$, the Vandermonde determinant is defined as

$$V(\mathbf{M}) = \prod_{1 \le k < \ell \le n} (m_k - m_\ell)\,. \tag{1}$$

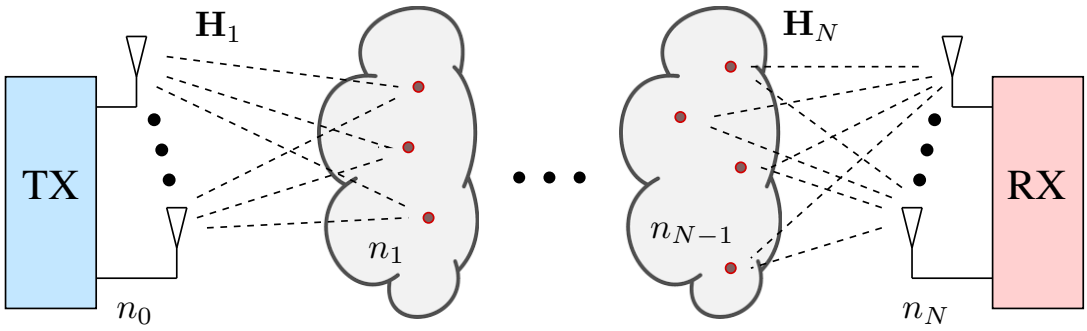

Fig. 1. Scattering channel representation.

B. Special functions

The Meijer-G function is defined as the line integral

$$G_{p,q}^{m,n}\left(\left.\begin{matrix}\mathbf{a}\\ \mathbf{b}\end{matrix}\right| z\right) = \frac{1}{2\pi i}\int_L \frac{\prod_{j=1}^{m}\Gamma(b_j-s)\prod_{j=1}^{n}\Gamma(1-a_j+s)z^s}{\prod_{j=m+1}^{q}\Gamma(1-b_j+s)\prod_{j=n+1}^{p}\Gamma(a_j-s)}\,\mathrm{d}s$$

where $\mathbf{a} = [a_1, \ldots, a_p]$, $\mathbf{b} = [b_1, \ldots, b_q]$, $\Gamma(s)$ is the Gamma function and the parameters m, n, p, q are integers [29, Ch. 8]. Moreover, L represents one among three suitable integration paths in the complex plane, selected according to the respective values of the integers m, n, p, q and the value of the variable z, as detailed in [29, 9.302].

C. Random variables

The probability density function (pdf) of the random variable a is denoted by $f_a(a)$, while its cumulative distribution function (CDF) by $F_a(a)$. Moreover, $\mathbb{E}_a[\cdot]$ represents the expectation operator with respect to the random variable a.

III. Channel Model

Let us consider a source-destination pair of multiple-antenna equipped nodes communicating through a wireless MIMO channel with $N-1$ independent scattering clusters (see Figure 1). Let us denote by n_0 and n_N the number of antennas at the source and destination, respectively. We

assume a memoryless block fading channel with block length equal to n_c channel uses. Then the signal received at the destination can be written as

$$\mathbf{Y} = \sqrt{\alpha}\mathbf{H}\mathbf{X} + \mathbf{N} \tag{2}$$

where the $n_N \times n_c$ matrix $\mathbf{Y}$ represents the output, the $n_0 \times n_c$ matrix $\mathbf{X}$ is the channel input, the $n_N \times n_0$ matrix $\mathbf{H}$ is the channel matrix, and $\mathbf{N}$ represents the matrix of AWGN noise with i.i.d. entries having zero mean and variance $\mathcal{N}_0$. For simplicity, in the following we assume $\mathcal{N}_0 = 1$.

Assuming no CSI at the transmitter, the available transmit power is uniformly distributed over all the n_0 antennas, hence $\mathbf{X}$ is modeled as a random matrix with i.i.d. entries and covariances

$$\mathbb{E}_{\mathbf{X}}[\mathbf{X}\mathbf{X}^{\mathsf{H}}] = \frac{\mathcal{P}n_c}{n_0}\mathbf{I}\,, \;\; \mathbb{E}_{\mathbf{X}}[\mathbf{X}^{\mathsf{H}}\mathbf{X}] = \mathcal{P}\mathbf{I}$$

where $\mathcal{P}$ is the total transmitted energy per channel use.

In our scenario we assume that $\mathbf{X}$ and $\mathbf{H}$ are independent and each cluster is composed of n_i independent scatterers, $i = 1, \ldots, N-1$. The random channel matrix, $\mathbf{H}$, is also referred to as *multiple-scattering channel matrix* and can be expressed as

$$\mathbf{H} = \mathbf{H}_N \cdots \mathbf{H}_1\,, \tag{3}$$

where matrices $\mathbf{H}_i$ are independent across i due to the independence of the scattering stages, and the generic matrix $\mathbf{H}_i$ has size $n_i \times n_{i-1}$. Such matrices are complex random with i.i.d. entries whose real and imaginary parts are independent and have a standard normal distribution [30]:

$$f_{\mathbf{H}_i}(\mathbf{H}_i) = \mathrm{e}^{-\mathsf{Tr}\{\mathbf{H}_i\mathbf{H}_i^{\mathsf{H}}\}}\pi^{-n_i n_{i-1}}\,. \tag{4}$$

Given the communication system under study, in this work we consider n_0 to be smaller than or equal to any n_i, with $i = 1, \ldots, N$. Then we further define auxiliary variables capturing the possible difference in spatial degrees of freedom/scattering richness at each cluster, namely $\nu_i = n_i - n_0\,, i = 1, \ldots, N$, which by assumption are non-negative integers.

The energy-normalization constant α can be written as

$$\alpha = \frac{n_0 n_N}{\mathsf{Tr}\{\mathbb{E}_{\mathbf{H}}[\mathbf{H}\mathbf{H}^{\mathsf{H}}]\}}\,. \tag{5}$$

Note that for the multiple-scattering channel in (3)

$$\begin{aligned}\mathsf{Tr}\{\mathbb{E}_{\mathbf{H}}[\mathbf{H}\mathbf{H}^{\mathsf{H}}]\} &= \mathsf{Tr}\{\mathbb{E}_{\mathbf{H}}[\mathbf{H}_N\cdots\mathbf{H}_1\mathbf{H}_1^{\mathsf{H}}\cdots\mathbf{H}_N^{\mathsf{H}}]\}\\ &= n_0\mathsf{Tr}\{\mathbb{E}_{\mathbf{H}}[\mathbf{H}_N\cdots\mathbf{H}_2\mathbf{H}_2^{\mathsf{H}}\cdots\mathbf{H}_N^{\mathsf{H}}]\}\\ &= \prod_{i=0}^{N-1} n_i\mathsf{Tr}\{\mathbb{E}_{\mathbf{H}}[\mathbf{H}_N\mathbf{H}_N^{\mathsf{H}}]\}\\ &= \prod_{i=0}^{N} n_i\,. \end{aligned} \tag{6}$$

It follows that

$$\alpha = \prod_{i=1}^{N-1}\frac{1}{n_i}\,. \tag{7}$$

As an example, if $N=1$ and $\mathbf{H}$ has i.i.d. Gaussian complex entries with zero mean and unit variance, we have $\alpha=1$ and, having assumed $\mathcal{N}_0=1$, the overall SNR of the system is $\mathcal{P}$.

Before proceeding into the information- and communication-theoretic investigation, we provide a comprehensive statistical analysis of the spectrum of the channel matrix in (3), which constitutes the basis of our subsequent findings.

IV. Spectral Analysis of Random Matrix Products

This section is devoted to the spectral analysis of Hermitian products of random matrices. It is articulated into two main subsections: the first one provides eigenvectors and eigenvalues statistics, while the second reports the *generalized variance* of the channel matrix in (3), as well as relevant integral transforms of the matrix spectrum.

A. Eigenvalue Decomposition and Its Properties

Let us consider the matrix $\mathbf{H}$ in (3), and the eigenvalue decomposition of its full-rank[3] Gram matrix, namely, $\mathbf{H}^{\mathsf{H}}\mathbf{H}=\mathbf{U}^{\mathsf{H}}\mathbf{\Lambda}\mathbf{U}$. This is an instance of a matrix with eigenvectors that, arranged as the columns of the n_0-dimensional square matrix $\mathbf{U}$, are jointly uniformly distributed on the group of the unitary matrices, $\mathcal{U}(n_0)$. This can be proven as done in the following proposition.

Proposition 4.1: Given a matrix product as in (3), its full-rank Gram matrix $\mathbf{H}^{\mathsf{H}}\mathbf{H}=\mathbf{U}^{\mathsf{H}}\mathbf{\Lambda}\mathbf{U}$ is unitarily invariant, i.e., $f_{\mathbf{H}^{\mathsf{H}}\mathbf{H}}(\widetilde{\mathbf{U}}^{\mathsf{H}}\mathbf{H}^{\mathsf{H}}\mathbf{H}\widetilde{\mathbf{U}}) = f_{\mathbf{H}^{\mathsf{H}}\mathbf{H}}(\mathbf{H}^{\mathsf{H}}\mathbf{H})$, for any choice of $\widetilde{\mathbf{U}}\in\mathcal{U}(n_0)$.

[3]Since we assumed $n_0\le n_N$, the number of non-zero singular values of $\mathbf{H}$ is n_0, thus its full-rank Gram matrix is of size n_0.

Moreover, $\mathbf{U}$ follows the Haar distribution [31, Formula (2.7)] and it is independent of $\mathbf{\Lambda}$, the diagonal matrix of the eigenvalues of $\mathbf{H}^{\mathsf{H}}\mathbf{H}$.

The proof of the above proposition follows directly from the observation that matrices $\mathbf{H}_i$ are bi-unitarily invariant by virtue of [31, Example 2.4], i.e., their pdf does not vary under left and/or right multiplication by a unitary matrix. As a consequence, the full-rank Gram matrix $\mathbf{H}^{\mathsf{H}}\mathbf{H} = \mathbf{H}_1^{\mathsf{H}}\mathbf{A}\mathbf{H}_1$ is unitarily invariant for any $\mathbf{A}$, and in particular for $\mathbf{A} = \mathbf{H}_2^{\mathsf{H}} \cdot \ldots \cdot \mathbf{H}_N^{\mathsf{H}}\mathbf{H}_N \cdot \ldots \cdot \mathbf{H}_2$.

The joint and marginal eigenvalue distributions of $\mathbf{H}^{\mathsf{H}}\mathbf{H}$ have been characterized, respectively, in [32] and in [1]. In particular, the joint law of the unordered n_0 eigenvalues of $\mathbf{H}^{\mathsf{H}}\mathbf{H}$ can be written as [32]

$$f_{\mathbf{\Lambda}}(\mathbf{\Lambda}) = \frac{1}{\mathcal{Z}} V(\mathbf{\Lambda}) |\mathbf{G}(\mathbf{\Lambda})| \,, \tag{8}$$

where the normalizing constant is given by [1, Eq.(21)]: $\mathcal{Z} = n_0! \prod_{i=1}^{n_0} \prod_{\ell=0}^{N} \Gamma(i+\nu_\ell)$, and $\mathbf{G}(\mathbf{\Lambda})$ is an $n_0 \times n_0$ matrix with generic entry

$$[\mathbf{G}(\mathbf{\Lambda})]_{i,j} = G_{0,N}^{N,0}\left(\begin{array}{c} - \\ \nu_N, \ldots, \nu_2, \nu_1 + i - 1 \end{array} \middle| \lambda_j \right) \,,$$

for $i, j = 1, \ldots, n_0$.

Let us now define the $n_0 \times n_0$ auxiliary matrix $\mathbf{A}_h$, with entries

$$[\mathbf{A}_h]_{i,j} = \Gamma(\nu_1 + i + j + h - 1) \prod_{\ell=2}^{N} \Gamma(\nu_\ell + j + h) \,, \tag{9}$$

where h is any integer number for which (9) takes meaningful values. We first observe that

$$|\mathbf{A}_0| = \frac{\mathcal{Z}}{n_0!} \tag{10}$$

The proof is reported in Appendix C. Also, drawing on [33, Theorem I], the following proposition holds.

Proposition 4.2: The marginal density of a single, unordered eigenvalue λ of $\mathbf{H}^{\mathsf{H}}\mathbf{H}$ is given by:

$$f_\lambda(\lambda) = \frac{1}{n_0} \mathsf{Tr}\left\{ \mathbf{A}_0^{-1} \mathbf{G}_1(\lambda) \right\} \tag{11}$$

where

$$[\mathbf{G}_1(\lambda)]_{i,j} = \lambda^{j-1} G_{0,N}^{N,0}\left(\begin{array}{c} - \\ \nu_N, \ldots, \nu_2, \nu_1 + i - 1 \end{array} \middle| \lambda \right) \,.$$

The CDF of a single, unordered eigenvalue λ of $\mathbf{H}^{\mathsf{H}}\mathbf{H}$ is given by

$$F_\lambda(\lambda) = \frac{1}{n_0} \mathsf{Tr}\left\{ \mathbf{A}_0^{-1} \mathbf{G}_2(\lambda) \right\} \tag{12}$$

where

$$[\mathbf{G}_2(\lambda)]_{i,j} = G_{1,N+1}^{N,1}\left(\begin{array}{c} 1 \\ \nu_N+j,\ldots,\nu_2+j,\nu_1+i+j-1,0 \end{array} \Big| \lambda \right). \tag{13}$$

Proof: The marginal density of a single unordered eigenvalue, can be obtained by integrating (8) w.r.t. all eigenvalues but one. This can be done by exploiting [33, Theorem I], which provides the result of the integration in terms of matrices $\mathbf{G}_1(\lambda)$ and $\mathbf{A}_0$, with $\mathbf{A}_0$ given by

$$\mathbf{A}_0 = \int_0^{+\infty} \mathbf{G}_1(\lambda)\,\mathrm{d}\lambda\,.$$

Its closed-form expression can be obtained from either [32, A.2], or by setting $h = 0$ in (9). The CDF in (12) can be obtained by integrating (11). The matrix $\mathbf{G}_2(\lambda)$, given by

$$\mathbf{G}_2(\lambda) = \int_0^{\lambda} \mathbf{G}_1(x)\,\mathrm{d}x\,, \tag{14}$$

can be written as in (13) by exploiting the properties of the Meijer-G function [29, (7.811.2)]. ■

Notice that (11) differs from the expression in [1, Formula (52)], which is based on the classical approach of k-point correlation functions for the density of an arbitrary subset of $k < n_0$ eigenvalues of a given random matrix. In particular, while (11) includes a single Meijer function only, the expression in [1] involves products of two Meijer functions. With regard to the moments of the unordered eigenvalue, we refer the reader to [1, Formula (55)], which holds for both integer and non-integer moment order.

A graphical representation of the CDF and the pdf of an unordered eigenvalue of $\mathbf{H}^{\mathsf{H}}\mathbf{H}$ is provided in Figures 2 and 3, respectively. The results are shown for a varying number of clusters ($N = 1,\ldots,6$), and $n_i = 4$ for any $i = 0,\ldots,4$. It can be noticed that the higher the number of stages in the channel matrix, the larger the range of possible values taken by the generic eigenvalue. In particular, as N grows, the pdf curve tends to resemble a straight line in a double-logarithmic plot. This is consistent with the trend observed in the SISO case in [34, Formula (8) and Fig. 1], where the pdf of the product of N independent Rayleigh-distributed random variables is derived. Therein, it is numerically shown that for $N = 5$, the pdf resembles a power law. Another relevant study to compare to is [3], where large-sized matrices, are investigated in the case of both a finite and an infinite number of *(unitarily invariant)* matrix factors. We remark however that a detailed analysis of the marginal pdf in (11) as N grows large, would require a rigorous investigation of the asymptotic behavior of the Meijer-G function, for which no results are available in the literature and which is subject of ongoing work.

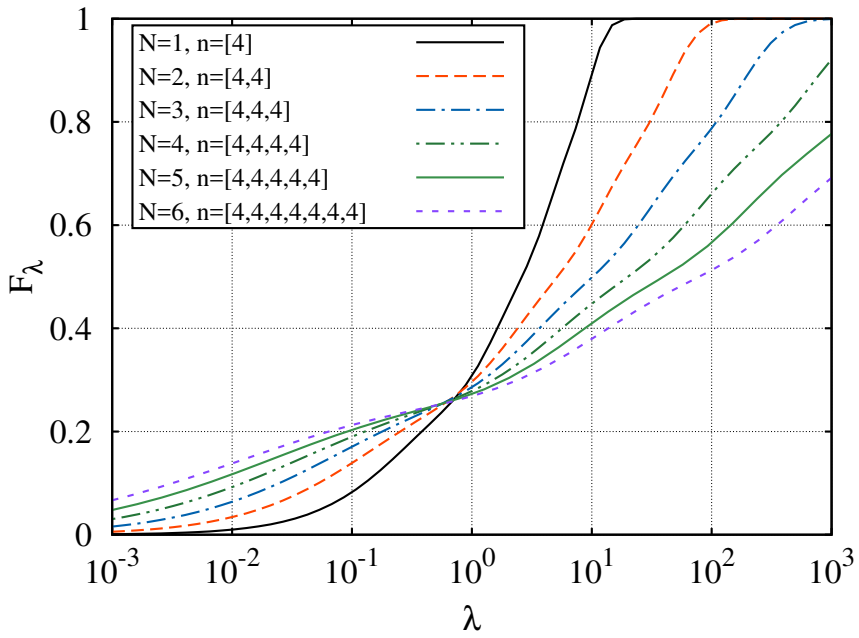

Fig. 2. Cumulative distribution of a single unordered eigenvalue of a multiple-scattering channel, for $n_i = 4$, $i = 0, \ldots, N$, and N ranging between 1 and 6.

A characterization of the extremal eigenvalues of $\mathbf{H}^{\mathsf{H}}\mathbf{H}$ is also provided in terms of their CDFs in the following proposition, which relies on [35].

Proposition 4.3: The CDF of the maximum eigenvalue $\lambda_{\max}$ of $\mathbf{H}^{\mathsf{H}}\mathbf{H}$ is given by:

$$F_{\lambda_{\max}}(\lambda) = \frac{|\mathbf{G}_2(\lambda)|}{|\mathbf{A}_0|}\,, \tag{15}$$

where $\mathbf{G}_2(\lambda)$ is given by (13). The pdf of the maximum eigenvalue is given by

$$f_{\lambda_{\max}}(\lambda) = \frac{|\mathbf{G}_2(\lambda)|}{|\mathbf{A}_0|}\mathsf{Tr}\{\mathbf{G}_2(\lambda)^{-1}\mathbf{G}_1(\lambda)\}\,. \tag{16}$$

In turn, the CDF and pdf of the minimum eigenvalue $\lambda_{\min}$ of $\mathbf{H}^{\mathsf{H}}\mathbf{H}$ can be written as

$$F_{\lambda_{\min}}(\lambda) = 1 - \frac{|\mathbf{G}_3(\lambda)|}{|\mathbf{A}_0|}, \tag{17}$$

and

$$f_{\lambda_{\min}}(\lambda) = \frac{|\mathbf{G}_3(\lambda)|}{|\mathbf{A}_0|}\mathsf{Tr}\{\mathbf{G}_3(\lambda)^{-1}\mathbf{G}_1(\lambda)\}, \tag{18}$$

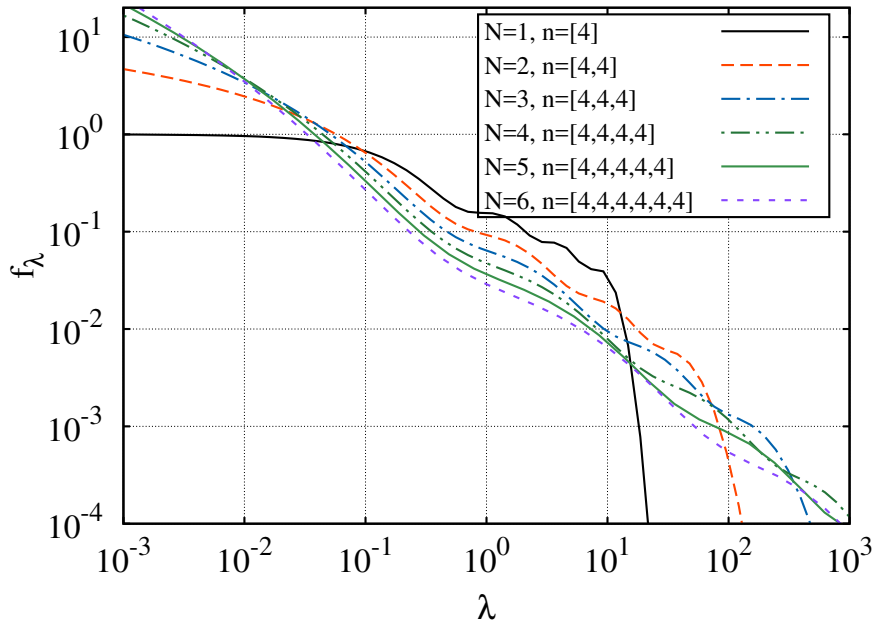

Fig. 3. Probability density function of a single unordered eigenvalue of a multiple-scattering channel, for $n_i = 4$, $i = 0, \ldots, N$, and N ranging between 1 and 6.

where

$$[\mathbf{G}_3(\lambda)]_{i,j} = G_{1,N+1}^{N+1,0}\left(\begin{array}{c} 1 \\ 0,\nu_N+j,\ldots,\nu_2+j,\nu_1+i+j-1 \end{array} \Big| \lambda \right) .$$

Proof: $F_{\lambda_{\max}}(\lambda)$ can be derived by following a similar approach to that adopted for the proof of [36, Theorem I]. Indeed, recall that the joint pdf of the ordered eigenvalues can be obtained from the unordered one given in (66), by multiplying it by $n_0!$ and taking into account that the ordered law, i.e.,

$$f_{\mathbf{\Lambda}}^{\mathrm{ord}}(\mathbf{\Lambda}) = \frac{|\mathbf{G}(\mathbf{\Lambda})|}{|\mathbf{A}_0|} V(\mathbf{\Lambda}) \,, \tag{19}$$

is defined over the domain[4] $\{0 \leq \lambda_1 < \lambda_2 < \ldots < \lambda_{n_0} < +\infty\}$. By definition, $F_{\lambda_{\max}}(\lambda) = \mathbb{P}\left(\lambda_{n_0} \leq \lambda\right)$, henceforth

$$F_{\lambda_{\max}}(\lambda) = \int_{\mathcal{D}} f_{\mathbf{\Lambda}}^{\mathrm{ord}}(\mathbf{\Lambda}) \, \mathrm{d}\mathbf{\Lambda} \,, \tag{20}$$

[4]We herein implicitly assume the eigenvalues to follow an increasing order, but all the statements hold also for a set of eigenvalues following a decreasing order.

where $\mathcal{D} = \{\mathbf{\Lambda} \in (\mathbb{R}^+)^{N_0} | \lambda_i \leq \lambda, i = 1, \ldots, n_0\}$. By virtue of [36, Lemma I], (20) can be equivalently written as (15). The pdf $f_{\lambda_{\max}}(\lambda)$ is obtained by computing the derivative of $F_{\lambda_{\max}}(\lambda)$ in (15). To do so, we exploit Jacobi's formula [37]:

$$\frac{\mathrm{d}}{\mathrm{d}z}|\mathbf{M}| = |\mathbf{M}|\mathsf{Tr}\left\{\mathbf{M}^{-1}\frac{\mathrm{d}\mathbf{M}}{\mathrm{d}z}\right\}, \tag{21}$$

getting

$$\begin{aligned} f_{\lambda_{\max}}(\lambda) &= \frac{\mathrm{d}}{\mathrm{d}\lambda}F_{\lambda_{\max}}(\lambda) \\ &= \frac{1}{|\mathbf{A}_0|}\frac{\mathrm{d}}{\mathrm{d}\lambda}|\mathbf{G}_2(\lambda)| \\ &= \frac{|\mathbf{G}_2(\lambda)|}{|\mathbf{A}_0|}\mathsf{Tr}\left\{\mathbf{G}_2(\lambda)^{-1}\frac{\mathrm{d}}{\mathrm{d}\lambda}\mathbf{G}_2(\lambda)\right\}. \end{aligned} \tag{22}$$

At last, from (14) we observe that the derivative of $\mathbf{G}_2(\lambda)$ is $\mathbf{G}_1(\lambda)$. In order to get an expression for $F_{\lambda_{\min}}(\lambda) = 1 - \mathbb{P}(\lambda_1 > \lambda)$, we first exploit [35, Eq. (7)], using (19), so that we get

$$F_{\lambda_{\min}}(\lambda) = 1 - \int_{\widetilde{\mathcal{D}}} f_{\mathbf{\Lambda}}^{\mathrm{ord}}(\mathbf{\Lambda})\,\mathrm{d}\mathbf{\Lambda}, \tag{23}$$

with $\widetilde{\mathcal{D}} = \{\mathbf{\Lambda} \in (\mathbb{R}^+)^{n_0} | \lambda_i > \lambda, i = 1, \ldots, n_0\}$. Then we apply [38, Corollary I] to obtain (17). Here again,

$$\mathbf{G}_3(\lambda) = \int_{\lambda}^{+\infty} \mathbf{G}_1(x)\,\mathrm{d}x, \tag{24}$$

can be written in closed form via [29, (7.811.3)], as reported in the proposition statement. The pdf $f_{\lambda_{\min}}(\lambda)$ can be obtained by deriving (17) and applying again the property in (21). In this case, however, according to (24) the derivative of $\mathbf{G}_3(\lambda)$ is given by $-\mathbf{G}_1(\lambda)$. ■

The CDF of the maximum and minimum eigenvalue of $\mathbf{H}^{\mathsf{H}}\mathbf{H}$ is depicted in Figure 4 for $N = 2$, and $n_0 = 4$, $n_1 = 5$ and $n_2 = 6$. The CDF of a single, unordered eigenvalue has been plotted too for completeness.

B. Generalized Variance and Spectral Transforms

This subsection is devoted to the investigation of the so-called *generalized variance*, given by the Gram determinant of a random matrix. We hereinafter provide the expression for the moments of $|\mathbf{H}^{\mathsf{H}}\mathbf{H}|$, and for its logarithm. We conclude the subsection by evaluating in closed form the Shannon transform of $\mathbf{H}^{\mathsf{H}}\mathbf{H}$, which is an integral transform largely adopted in communication

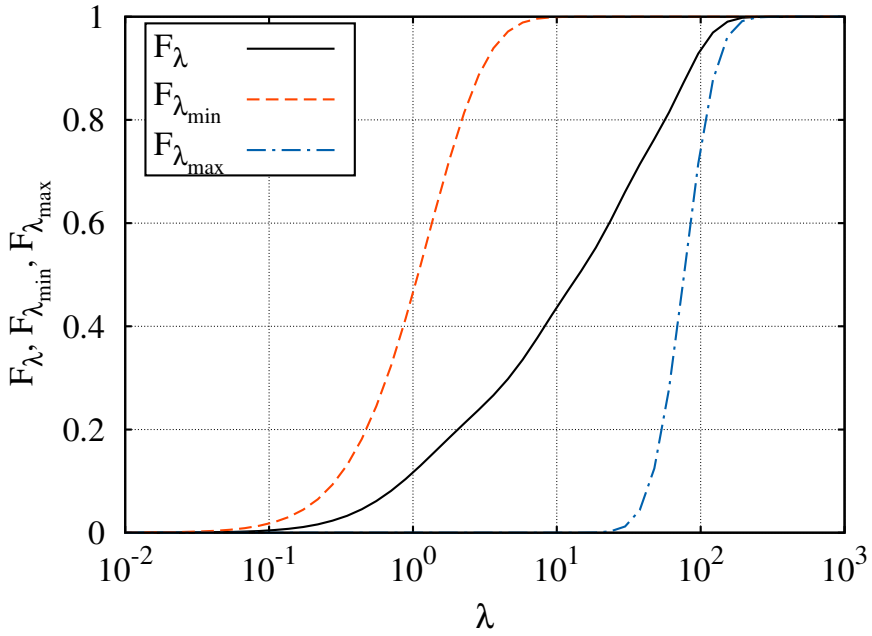

Fig. 4. Cumulative distribution of the maximum, the minimum, and of a single unordered eigenvalue of a multiple-scattering channel, with $N = 2$ scattering stages, $n_0 = 4, n_1 = 5$, and $n_2 = 6$.

theory[5]. The closed-form expression for the Shannon transform of $\mathbf{H}^{\mathsf{H}}\mathbf{H}$ will be useful to derive our results in Section VI.

Proposition 4.4: The moments of $|\mathbf{H}^{\mathsf{H}}\mathbf{H}|$ can be expressed as

$$\mathbb{E}_{\mathbf{H}}[|\mathbf{H}^{\mathsf{H}}\mathbf{H}|^h] = \frac{|\mathbf{A}_h|}{|\mathbf{A}_0|} \qquad h \in \mathbb{N}\,. \tag{25}$$

Proof: Let us first recall that $|\mathbf{H}^{\mathsf{H}}\mathbf{H}| = |\mathbf{\Lambda}|$. Then, using (8), we have:

$$\begin{aligned}\mathbb{E}_{\mathbf{H}}[|\mathbf{H}^{\mathsf{H}}\mathbf{H}|^h] &= \frac{1}{n_0!|\mathbf{A}_0|}\int_{(\mathbb{R}^+)^{n_0}} V(\mathbf{\Lambda})|\mathbf{G}(\mathbf{\Lambda})||\mathbf{\Lambda}|^h \,\mathrm{d}\mathbf{\Lambda} \\ &= \frac{|\mathbf{A}_h|}{|\mathbf{A}_0|},\end{aligned}$$

[5]The Shannon transform, along with the η-transform that we also provide for completeness, are rigorously defined with respect to the laws of non negative random variables. In this work, as customary in the literature, by transform of an Hermitian random matrix we mean the transform of its marginal unordered eigenvalue density, since we deal with finite-dimensional random matrices.

by virtue of [38, Corollary I]. Note that, by applying [29, 7.811.4], (9) can be rewritten as

$$[\mathbf{A}_h]_{i,j} = \int_{\mathbb{R}^+} \lambda^{j-1+h} G_{0,N}^{N,0} \left(\begin{matrix} - \\ \nu_N, \ldots, \nu_2, \nu_1+i-1 \end{matrix} \middle| \lambda \right) \mathrm{d}\lambda \,.$$

■

From Proposition 4.4, the Corollary below follows.

Corollary 4.1:

$$\mathbb{E}_{\mathbf{H}}[\ln |\mathbf{H}^{\mathsf{H}}\mathbf{H}|] = \mathsf{Tr}\left\{ \mathbf{A}_0^{-1} \widetilde{\mathbf{A}}_0 \right\} , \tag{26}$$

where $\widetilde{\mathbf{A}}_0$ is a square matrix of size n_0, with elements given by

$$\left[\widetilde{\mathbf{A}}_0\right]_{i,j} = [\mathbf{A}_0]_{i,j} \left[\sum_{t=1}^{\nu_1+i+j-2} \frac{1}{t} + \sum_{\ell=2}^{N} \sum_{t=1}^{\nu_\ell+j-1} \frac{1}{t} - N\gamma \right] . \tag{27}$$

In the above equation, γ is the Euler-Mascheroni constant.

Proof: In order to prove the corollary, we can write:

$$\begin{aligned} \mathbb{E}_{\mathbf{H}} \left[\ln |\mathbf{H}^{\mathsf{H}}\mathbf{H}|\right] &= \frac{\mathrm{d}}{\mathrm{d}s} \mathbb{E}_{\mathbf{H}} \left[\exp(s \ln |\mathbf{H}^{\mathsf{H}}\mathbf{H}|)\right] \Big|_{s=0} \\ &= \frac{\mathrm{d}}{\mathrm{d}s} \mathbb{E}_{\mathbf{H}} \left[|\mathbf{H}^{\mathsf{H}}\mathbf{H}|^s\right] \Big|_{s=0} \\ &= \frac{1}{|\mathbf{A}_0|} \frac{\mathrm{d}}{\mathrm{d}s} |\mathbf{A}_s| \Big|_{s=0} \end{aligned} \tag{28}$$

where in the last line we exploited Proposition 4.4. To compute the derivative of a matrix determinant, we apply the property in (21) and obtain

$$\begin{aligned} \frac{\mathrm{d}}{\mathrm{d}s} |\mathbf{A}_s| \Big|_{s=0} &= |\mathbf{A}_s| \mathsf{Tr}\left\{ \mathbf{A}_s^{-1} \frac{\mathrm{d}}{\mathrm{d}s} \mathbf{A}_s \right\} \Big|_{s=0} \\ &= |\mathbf{A}_0| \mathsf{Tr}\left\{ \mathbf{A}_0^{-1} \widetilde{\mathbf{A}}_0 \right\} \end{aligned} \tag{29}$$

where $\widetilde{\mathbf{A}}_0 = \frac{\mathrm{d}}{\mathrm{d}s}\mathbf{A}_s\big|_{s=0}$. The generic i,j-th entry of $\widetilde{\mathbf{A}}_0$ is given by:

$$\begin{aligned}\left[\widetilde{\mathbf{A}}_0\right]_{i,j} &= \frac{\mathrm{d}}{\mathrm{d}s}\Gamma(\nu_1+i+j+s-1)\prod_{\ell=2}^{N}\Gamma(\nu_\ell+j+s)\Big|_{s=0} \\ &= \Gamma(\nu_1+i+j-1)\prod_{\ell=2}^{N}\Gamma(\nu_\ell+j)\cdot \\ &\quad \left[-\gamma+\sum_{t=1}^{\nu_1+i+j-2}\frac{1}{t}+\sum_{\ell=2}^{N}\left(-\gamma+\sum_{t=1}^{\nu_\ell+j-1}\frac{1}{t}\right)\right] \\ &= [\mathbf{A}_0]_{i,j}\left[\sum_{t=1}^{\nu_1+i+j-2}\frac{1}{t}+\sum_{\ell=2}^{N}\sum_{t=1}^{\nu_\ell+j-1}\frac{1}{t}-N\gamma\right].\end{aligned} \tag{30}$$

By substituting (30) and (29) in (28), we obtain the assertion. ■

As mentioned, we conclude the section by providing the expression of the Shannon transform of $\mathbf{H}^{\mathsf{H}}\mathbf{H}$, which is related to the mutual information.

The Shannon transform [31, Def. 2.12] of the $n_0 \times n_0$ random matrix $\mathbf{H}^{\mathsf{H}}\mathbf{H}$ is given by

$$\mathcal{V}(\beta, n_0) = \mathbb{E}_\lambda\left[\ln(1+\beta\lambda)\right]$$

where λ is any unordered eigenvalue of $\mathbf{H}^{\mathsf{H}}\mathbf{H}$. In the case of our multiple-scattering channel, the following proposition holds.

Proposition 4.5: The Shannon transform of $\mathbf{H}^{\mathsf{H}}\mathbf{H}$ for the multiple-scattering channel in (3) is given by:

$$\mathcal{V}(\beta, n_0) = \frac{1}{n_0}\mathsf{Tr}\{\mathbf{A}_0^{-1}\mathbf{G}_4(\beta)\} \tag{31}$$

where

$$[\mathbf{G}_4(\beta)]_{i,j} = G_{2,N+2}^{N+2,1}\left(\begin{matrix}0,1\\ 0,0,\nu_N+j,\ldots,\nu_2+j,\nu_1+i+j-1\end{matrix}\Big|\frac{1}{\beta}\right)$$

with

$$\beta = \frac{\mathcal{P}\alpha}{n_0}. \tag{32}$$

Proof: The assertion is obtained by replacing (11) in the definition of the Shannon transform given above, by writing $\ln(1+\beta\lambda)$ in terms of a Meijer-G and by exploiting the properties of the Meijer-G functions [29]. ■

For the sake of completeness, we also derive the η-transform [31, Def. 2.11], defined as

$$\eta(\beta, n_0) = \mathbb{E}_\lambda\left[(1+\beta\lambda)^{-1}\right].$$

By replacing once again (11) in the above definition and by exploiting [29, 7.811.5], we obtain:

$$\eta\left(\beta, n_0\right) = \frac{1}{n_0}\mathsf{Tr}\{\mathbf{A}_0^{-1}\mathbf{G}_5(\beta)\} \tag{33}$$

where

$$\left[\mathbf{G}_5(\beta)\right]_{i,j} = G_{1,N+1}^{N+1,1}\left(\begin{array}{l} 1 \\ 1,\nu_N+j,\ldots,\nu_2+j,\nu_1+i+j-1 \end{array}\Big|\frac{1}{\beta}\right).$$

V. Error Exponents and Cutoff Rate

To evaluate the error exponents for the channel under study, we refer to the matrix-valued transmission model in (2). Assuming each codeword to span over $n_b n_c$ channel uses, we collect n_b independent realizations of (3). The average error probability achievable by a code of rate R with maximum likelihood decoding can be bounded as [16, Ch. 7]:

$$P_e \leq \left(\frac{2\mathrm{e}^{r\delta}}{\chi}\right)^2 \exp\left(-n_b n_c E(f_{\mathbf{X}}(\mathbf{X}), R, n_c)\right), \tag{34}$$

where $r, \delta > 0$, $\chi \approx \frac{\delta}{\sqrt{2\pi n_b \sigma_\chi^2}}$, $\sigma_\chi^2 = \mathbb{E}_{\mathbf{X}}\left[\left(\|\mathbf{X}\|^2 - n_c\mathcal{P}\right)^2\right]$, $E(f_{\mathbf{X}}(\mathbf{X}), R, n_c)$ is the RCEE, and $f_{\mathbf{X}}(\mathbf{X})$ is the distribution of the channel input $\mathbf{X}$. The variable $\mathcal{P}$ denotes the average input-power constraint, i.e.,

$$\mathbb{E}_{\mathbf{X}}[\|\mathbf{X}\|^2] \leq n_c\mathcal{P} \tag{35}$$

for a given distribution of the input matrix $f_{\mathbf{X}}(\mathbf{X})$. The RCEE in (34) is given by

$$E(f_{\mathbf{X}}(\mathbf{X}), R, n_c) = \max_{0\leq\rho\leq 1}\left\{\max_{r\geq 0} -\frac{\ln\mathcal{E}}{n_c} - \rho R\right\}, \tag{36}$$

where $\mathcal{E}$ is defined as

$$\mathcal{E} \;=\; \mathbb{E}_{\mathbf{H}}\left[\int_{\mathbb{C}^{n_N\times n_c}} \mathbb{E}_{\mathbf{X}}\left[f(\mathbf{Y}|\mathbf{X},\mathbf{H})^{\frac{1}{1+\rho}}\mathrm{e}^{r(\|\mathbf{X}\|^2 - n_c\mathcal{P})}\right]^{1+\rho} \mathrm{d}\mathbf{Y}\right]. \tag{37}$$

Rigorously, random coding equally weights both good as well as bad codewords. An improved bound for the average error probability can be obtained by expurgating bad codewords from the code ensemble (see, e.g., [16]). Such an expurgating procedure leads to the following upper bound for the error probability

$$P_e \leq \exp\left(-n_b n_c E_e(f_{\mathbf{X}}(\mathbf{X}), R, n_c) + o(1)\right), \tag{38}$$

where

$$E_e(f_{\mathbf{X}}(\mathbf{X}), R, n_c) = \max_{0\leq\rho\leq 1}\left\{\max_{r\geq 0} -\frac{\ln\mathcal{E}_e}{n_c} - \rho R\right\} \tag{39}$$

is the EEE. $\mathcal{E}_e$ denotes the matrix integral

$$\mathcal{E}_e = \mathbb{E}_{\mathbf{H}}\left[\mathbb{E}_{\mathbf{X},\mathbf{X}'}\left[\mathrm{e}^{r(\|\mathbf{X}\|^2+\|\mathbf{X}'\|^2-2n_c\mathcal{P})}w(\mathbf{X},\mathbf{X}',\mathbf{H})^{\frac{1}{\rho}}\right]^{\rho}\right] \tag{40}$$

and

$$w(\mathbf{X},\mathbf{X}',\mathbf{H}) = \int_{\mathbb{C}^{n_N\times n_c}} \sqrt{f(\mathbf{Y}|\mathbf{X},\mathbf{H})f(\mathbf{Y}|\mathbf{X}',\mathbf{H})}\,\mathrm{d}\mathbf{Y}\,. \tag{41}$$

In (40), $\mathbf{X}'$ shares the same distribution as $\mathbf{X}$ and represents the input signal of good codewords. Note that, without CSI at the receiver, the expressions in (37) and (40) would depend on $f(\mathbf{Y}|\mathbf{X})$ and $f(\mathbf{Y}|\mathbf{X}')$ rather than on $f(\mathbf{Y}|\mathbf{X},\mathbf{H})$ and $f(\mathbf{Y}|\mathbf{X}',\mathbf{H})$. However, $f(\mathbf{Y}|\mathbf{X})$ and $f(\mathbf{Y}|\mathbf{X}')$ are difficult to evaluate, except for the case of uncorrelated Rayleigh fading, asymptotically analyzed in [23]. Notice also that the optimal distribution $f(\mathbf{X})$ would be the one that maximizes the error exponents (either $E(f_{\mathbf{X}}(\mathbf{X}),R,n_c)$ or $E_e(f_{\mathbf{X}}(\mathbf{X}),R,n_c)$). However, in the following, as usually done in the literature (see, e.g., [17], [19], [20] and references therein), we assume that $f_{\mathbf{X}}(\mathbf{X})$ follows a Gaussian distribution, i.e.,

$$f_{\mathbf{X}}(\mathbf{X}) = \mathrm{e}^{-\mathsf{Tr}\{\mathbf{Q}^{-1}\mathbf{X}\mathbf{X}^{\mathsf{H}}\}}|\pi\mathbf{Q}|^{-n_c}\,, \tag{42}$$

where the covariance matrix $\mathbf{Q} = \frac{1}{n_c}\mathbb{E}[\mathbf{X}\mathbf{X}^{\mathsf{H}}]$ should satisfy the average power constraint enforced in (35)

$$\mathbb{E}_{\mathbf{X}}[\|\mathbf{X}\|^2] = n_c\mathsf{Tr}\{\mathbf{Q}\} \le n_c\mathcal{P}.$$

This assumption simplifies the evaluation of the error exponent. Also, the Gaussian law for $\mathbf{X}$ is optimal if the rate R approaches the channel capacity.

When R is close to the capacity and CSI is available at the receiver but not at the transmitter, Uniform Power Allocation (UPA) across transmit antennas yields optimal performance in the presence of a unitarily invariant channel matrix [22]. Under UPA, the covariance matrix of the channel input is scalar. That is, it can be written as $\mathbf{Q} = p\mathbf{I}$ where

$$p = \frac{\mathcal{P}}{n_0}$$

represents the per-antenna transmit power, assuming the average power constraint is met with equality.

A. Random Coding Error Exponent

Theorem 5.1: For a block-fading channel as in (3), fed by a Gaussian input according to (42) with UPA (i.e., $\mathbf{Q} = p\mathbf{I}$), the RCEE related to an observation window of n_b independent fading blocks of n_c channel uses each, can be expressed as per (36) with[6]

$$\mathcal{E} = k \int_{(\mathbb{R}^+)^{n_0}} f_{\mathbf{\Lambda}}(\mathbf{\Lambda}) \left| \mathbf{I} + \frac{\alpha p}{(1+\rho)(1-pr)} \mathbf{\Lambda} \right|^{-n_c \rho} \mathrm{d}\mathbf{\Lambda}, \tag{43}$$

where we recall that $\mathbf{\Lambda}$ is the diagonal eigenvalue matrix and r is the parameter appearing in 34.

$$k = \frac{\mathrm{e}^{-r n_c \mathcal{P}(1+\rho)}}{(1-pr)^{n_c n_0 (1+\rho)}},$$

The proof can be found in [39]. Notice, however, that (43) slightly differs from [39, Formula (11)], where no constraint between the number of transmit and receive antennas was enforced, while our current analysis assumes $n_0 \leq n_N$.

Proposition 5.1: For a block-fading channel as in (3), the RCEE is given by (36) where

$$\mathcal{E} = \frac{k}{|\mathbf{A}_0|} \left| \mathbf{Z}\left(\frac{(1-pr)(1+\rho)}{\alpha p} \right) \right|, \tag{44}$$

and k is given in Theorem 5.1. The elements of the $n_0 \times n_0$ matrix $\mathbf{Z}(x)$ are given by

$$[\mathbf{Z}(x)]_{i,j} = \frac{G_{1,N+1}^{N+1,1}\left(\begin{array}{l} 1 \\ n_c\rho, \nu_N+j, \ldots, \nu_2+j, \nu_1+i+j-1 \end{array} \middle| x \right)}{\Gamma(n_c \rho)}.$$

Proof: The proof is provided in Appendix B. ■

The channel cutoff rate corresponding to the RCEE, according to [17, Eqs. (26-27)], can be written as

$$R_0 = -\frac{\log \mathcal{E}}{n_c}\Big|_{r=0,\rho=1},$$

for which a closed-form expression can be straightforwardly obtained from (44).

[6]We remark that our derivation, albeit slightly more compact, partially overlaps with the content of [17, Appendix A], where the analysis was focused on Rayleigh-faded channels.

B. Expurgated Error Exponent

Theorem 5.2: For a block-fading channel as in (2), fed by a Gaussian input according to (42) with UPA (i.e., $\mathbf{Q} = p\mathbf{I}$), the EEE related to an observation window of n_b independent fading blocks of n_c channel uses each, can be expressed as per (39) with

$$\mathcal{E}_e = k_e \int_{(\mathbb{R}^+)^{n_0}} f_{\mathbf{\Lambda}}(\mathbf{\Lambda}) \left| \mathbf{I} + \frac{\alpha p}{2\rho(1-pr)} \mathbf{\Lambda} \right|^{-n_c \rho} \mathrm{d}\mathbf{\Lambda} \tag{45}$$

where

$$k_e = \frac{\mathrm{e}^{-2rn_c\mathcal{P}\rho}}{(1-pr)^{2n_0 n_c \rho}}$$

Proof: The proof is given in Appendix A. ■

Proposition 5.2: For a block-fading channel as in (2), with channel matrix given by (3), the EEE is given by (45) where

$$\mathcal{E}_e = \frac{k_e}{|\mathbf{A}_0|} \left| \mathbf{Z}\left(\frac{2(1-pr)\rho}{\alpha p} \right) \right| , \tag{46}$$

and where k_e is defined in Theorem 5.2.

Proof: The proof is given in Appendix B. ■

C. Numerical Results

Here we briefly report on the behavior of the cutoff rate of a multiple-scattering MIMO channel, relying on our newly derived expression.

In Figure 5, we plot the cutoff rate as a function of the transmit power, in the case of random coding. We set $n_c = 9$ and $n_i = 4$, $i = 0, \ldots, N$ and we show the results for an increasing number of scattering clusters ($N = 1, \ldots, 6$). As expected, the cutoff rate increases with the transmit power, and decreases as the number of scattering clusters grows. In particular, we remark that, in the high-SNR region (i.e., beyond $20\,$dB), doubling the number of clusters N has a similar impact on the cutoff rate to that observed when reducing the transmitted power by $10\,$dB.

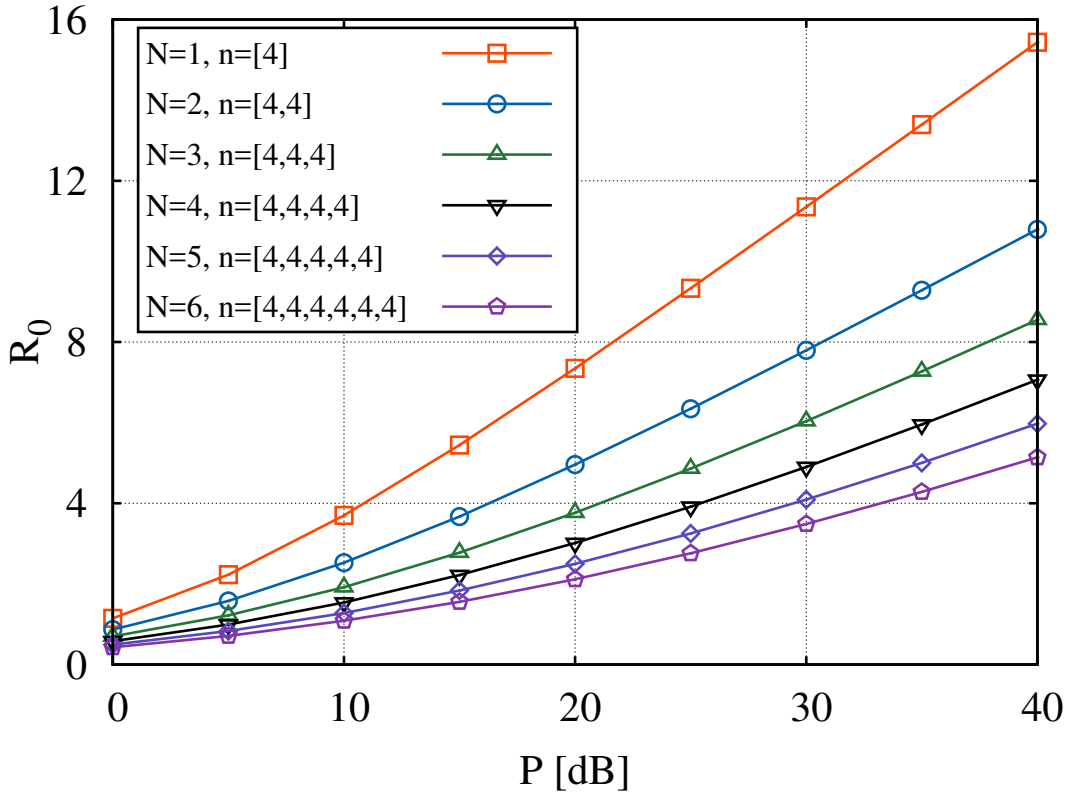

Fig. 5. Cutoff rate as a function of the transmit power for $n_c = 9$, $n_i = 4$, $i = 0, \ldots, N$, and N ranging between 1 and 6.

VI. Mutual Information and Sum Rate Analysis

When perfect CSI is available at the receiver, the ergodic mutual information achieved by optimal receive processing is given by [1]:

$$\begin{aligned} \mathcal{I}(\beta, n_0) &= \mathbb{E}_{\mathbf{H}}\left[\ln\left|\mathbf{I} + \beta \mathbf{H}^{\mathsf{H}}\mathbf{H}\right|\right] \\ &= \mathbb{E}_{\mathbf{\Lambda}}\left[\ln\left|\mathbf{I} + \beta \mathbf{\Lambda}\right|\right] \\ &= n_0 \mathbb{E}_{\lambda}\left[\ln\left(1 + \beta\lambda\right)\right] \\ &= n_0 \int_0^{\infty} \ln\left(1 + \beta\lambda\right) f_{\lambda}(\lambda)\, \mathrm{d}\lambda\,, \end{aligned} \tag{47}$$

where we recall that λ is the generic unordered eigenvalue of $\mathbf{H}^{\mathsf{H}}\mathbf{H}$. Notice that, although $\mathcal{I}$ depends on several system parameters, for simplicity in (47) we highlighted only the dependency

on the SNR and on the number of transmit antennas, n_0. f_λ too depends on several integer parameters, according to (11), however we preferred to highlight the dependency on n_0 only.

Assuming that a linear receiver is used instead of the optimal one, the system incurs some performance loss. The relationship between the optimal ergodic mutual information and the sum rate achieved by the MMSE receiver has been unveiled in [25]. Therein, compact expressions for achievable rates have been derived in the case of Rayleigh and Ricean-faded MIMO channels, under various assumptions on the spatial correlation.

In this section, we extend the analysis to the multiple-scattering channel matrix in (3). Furthermore, we analyse the case of ZF receiver, deriving in this last case upper and lower bounds following both the approaches proposed by Matthaiou *et al.* in [26], [27] and that of Jiang *et al.* in [28].

A. Optimal Receiver Performance

Using the definition of the Shannon transform and (47), we can write:

$$\mathcal{I}(\beta, n_0) = n_0 \mathcal{V}(\beta, n_0) \ . \tag{48}$$

B. Linear Receivers Sum Rate

Let us consider the MIMO communication channel described in (2) and that a linear filter is used at the receiver output. Under the assumption of independent stream decoding, the MIMO channel can be decomposed into n_0 parallel subchannels [40], with ρ_k denoting the instantaneous SINR corresponding to the k-th subchannel. Then the achievable sum rate can be written as

$$R \triangleq \sum_{k=1}^{n_0} \mathbb{E}_{\rho_k}[\ln(1+\rho_k)] \, . \tag{49}$$

The expression of ρ_k depends on the adopted receiving strategy (e.g., MMSE or ZF). Below we provide the exact closed-form expression for the achievable sum rate in the case of the MMSE receiver, and an upper and a lower bound in the case of the ZF receiver. Note that the results we present below are based on the eigenanalysis of $\mathbf{H}^{\mathsf{H}}\mathbf{H}$, rather than on the (cumbersome) statistics of ρ_k.

1) MMSE Performance Analysis: The MMSE filter for the signal in (2) is given by $\mathbf{F} = \mathbf{H}^{\mathsf{H}}(\mathbf{H}\mathbf{H}^{\mathsf{H}} + \mathbf{I}/\beta)^{-1}$, where β is as in (32). The k-th component of the filtered signal $\mathbf{F}\mathbf{y}$ has SINR given by [41, Ch. 6]: $\rho_k = \frac{1}{\left[\left(\mathbf{I}+\beta\mathbf{H}^{\mathsf{H}}\mathbf{H}\right)^{-1}\right]_{k,k}} - 1$. An explicit expression for the pdf of ρ_k is

only available in the canonical Rayleigh case, i.e., when $\mathbf{H}^{\mathsf{H}}\mathbf{H}$ is a central, uncorrelated Wishart matrix with n_N degrees of freedom [42]. However, by writing the term $[(\mathbf{I}+\beta\mathbf{H}^{\mathsf{H}}\mathbf{H})^{-1}]_{k,k}$ as [43]: $\left[\left(\mathbf{I}+\beta\mathbf{H}^{\mathsf{H}}\mathbf{H}\right)^{-1}\right]_{k,k} = \frac{\left|\mathbf{I}+\beta\mathbf{H}^{(k)\mathsf{H}}\mathbf{H}^{(k)}\right|}{\left|\mathbf{I}+\beta\mathbf{H}^{\mathsf{H}}\mathbf{H}\right|}$, where $\mathbf{H}^{(k)}$ is the matrix obtained by removing the k-th column from $\mathbf{H}$, and upon substitution of the above expression and of that of ρ_k in (49), we obtain [25]:

$$R^{\mathrm{MMSE}} = \sum_{k=1}^{n_0} \mathbb{E}_{\mathbf{H}}\left[\ln\left|\mathbf{I}+\beta\mathbf{H}^{\mathsf{H}}\mathbf{H}\right|\right] - \sum_{k=1}^{n_0} \mathbb{E}_{\mathbf{H}^{(k)}}\left[\ln\left|\mathbf{I}+\beta\mathbf{H}^{(k)\mathsf{H}}\mathbf{H}^{(k)}\right|\right] . \tag{50}$$

By using (47), the first term on the right hand side of (50) can be written as $n_0\mathcal{I}(\beta,n_0)$. The second term depends, instead, on the distribution of the matrix $\mathbf{H}^{(k)}$, which has size $n_N \times n_0 - 1$, and which, by virtue of (3), can be rewritten as $\mathbf{H}^{(k)} = \mathbf{H}_N \cdots \mathbf{H}_i \cdots \mathbf{H}_1^{(k)}$, where $\mathbf{H}_1^{(k)}$ is the matrix obtained by removing the k-th column from $\mathbf{H}_1$. Since the entries of $\mathbf{H}_1$ are i.i.d., we conclude that the term $W = \mathbb{E}_{\mathbf{H}^{(k)}}[\ln|\mathbf{I}+\beta\mathbf{H}^{(k)\mathsf{H}}\mathbf{H}^{(k)}|]$ does not depend on k. Moreover, noticing that, for each k, one of the transmit antennas is virtually switched off, it follows that (cfr. [25]) $W = \mathcal{I}(\beta, n_0-1)$. In conclusion,

$$\begin{aligned} R^{\mathrm{MMSE}} &= n_0\mathcal{I}(\beta,n_0) - n_0\mathcal{I}(\beta,n_0-1) \\ &= n_0^2\mathcal{V}(\beta,n_0) - n_0(n_0-1)\mathcal{V}(\beta,n_0-1) . \end{aligned}$$

From (51), it immediately follows that the availability of an explicit expression for the Shannon transform of the channel matrix allows for a closed-form evaluation of the sum rate in the MMSE case.

2) ZF Performance Bounds: For the sake of completeness, we also present an approximate analysis of the ZF filter, which constitutes a low-complexity alternative to the implementation of the linear MMSE filter and offers asymptotically equivalent sum-rate performance in the high-SNR regime. When the ZF filter is employed at the receiver, the SNR on the k-th sub-channel is given by: $\rho_k = \frac{\beta}{\left[\left(\mathbf{H}^{\mathsf{H}}\mathbf{H}\right)^{-1}\right]_{k,k}}$.

In the absence of an exact expression for the sum rate of a MIMO communication with ZF receiver, we work toward bounding R^{ZF}. At first, we exploit the bounds provided in [26], directly derived with reference to the sum rate, rather than on ρ_k, and collect related results in the following proposition.

Proposition 6.1: The sum rate achievable with a ZF receiver over a MIMO channel affected by Rayleigh fading, in the presence of multiple scattering, is upper bounded by [26, Thm.1][7]:

$$\begin{aligned} R^{\mathrm{ZF}} &\leq n_0 \ln\left(\mathbb{E}_\lambda\left[\lambda^{-1}\right]+\beta\right) + n_0 \mathbb{E}_{\mathbf{H}}\left[\ln|\mathbf{H}^{\mathsf{H}}\mathbf{H}|\right] - \sum_{k=1}^{n_0} \mathbb{E}_{\mathbf{H}^{(k)}}\left[\ln|\mathbf{H}^{(k)\mathsf{H}}\mathbf{H}^{(k)}|\right] \\ &= n_0 \ln\left(\mathbb{E}_\lambda\left[\lambda^{-1}\right]+\beta\right) + n_0 \mathbb{E}_{\mathbf{H}}\left[\ln|\mathbf{H}^{\mathsf{H}}\mathbf{H}|\right] - n_0 \mathbb{E}_{\mathbf{H}^{(1)}}\left[\ln\left|\mathbf{H}^{(1)\mathsf{H}}\mathbf{H}^{(1)}\right|\right] \end{aligned} \tag{51}$$

where we recall that matrix $\mathbf{H}^{(k)}$ is obtained from $\mathbf{H}$ by removing the k-th column, and that, due to the independence and identical distribution of the columns of $\mathbf{H}^{(k)}$, the average $\mathbb{E}_{\mathbf{H}^{(k)}}[\ln|\mathbf{H}^{(k)\mathsf{H}}\mathbf{H}^{(k)}|]$ does not depend on k. Its value can be computed by exploiting Corollary 4.1 and by noting that $\mathbf{H}^{(k)\mathsf{H}}\mathbf{H}^{(k)}$ has size $(n_0-1)\times(n_0-1)$. The expression of the first negative moment of λ can be found in [1, Eq. (59)].

The sum rate is, in turn, lower bounded by [26, Thm.3]:

$$R^{\mathrm{ZF}} \geq \sum_{k=1}^{n_0} \ln\left(1+\beta \mathrm{e}^{\phi_k}\right) = n_0 \ln\left(1+\beta \mathrm{e}^{\phi_1}\right) \tag{52}$$

where for any $k \in \{1,\ldots,n_0\}$, $\phi_k = \mathbb{E}_{\mathbf{H}}\left[\ln|\mathbf{H}^{\mathsf{H}}\mathbf{H}|\right] - \mathbb{E}_{\mathbf{H}^{(k)}}\left[\ln\left|\mathbf{H}^{(k)\mathsf{H}}\mathbf{H}^{(k)}\right|\right]$. Note that in (52) we exploited the fact that, due to the already recalled symmetries in the law of the $\mathbf{H}^{(k)}$'s, the actual value of ϕ_k does not depend on the index k. An explicit expression of (52) for the channel model at hand is obtained by replacing (26) in the expression of the ϕ_k's.

For the sake of completeness, we also report the upper [28, Eq. (6)] and lower [44, Eq. (8)] bounds to the SINR, both related to the smallest eigenvalue of $\mathbf{H}^{\mathsf{H}}\mathbf{H}$. I.e.,

$$\lambda_{\min}\beta \leq \rho_k \leq \frac{\lambda_{\min}\beta}{u}, \tag{53}$$

where u is a Beta random variable[8], hence $f_u(u) = (n_0-1)(1-u)^{n_0-2}$, $0 \leq u \leq 1$. From (53) and the fact that the bounds are independent of k, it follows that

$$R^{\mathrm{ZF}} \geq n_0 \mathbb{E}_{\lambda_{\min}} \ln\left(1+\lambda_{\min}\beta\right), \tag{54}$$

[7]This bound explicitly depends on the first negative moment of an unordered eigenvalue of the channel matrix; in case it does not exist, one can resort to the upper bound [26, Thm.2], which holds irrespectively from the availability of $\mathbb{E}_\lambda[\lambda^{-1}]$. We further notice that no new analytical results are to be derived in order to evaluate the mentioned bound in [26, Thm.2], which only requires the closed-form expression of the determinantal moments, provided in Corollary 4.1.

[8]With reference to the proof technique of [28, Lemma V.I], we notice that the rightmost inequality (53) holds for any unitarily invariant matrix, and thus in particular for (3). With regard to the leftmost one, it holds also for MMSE receivers.

while

$$R^{\mathrm{ZF}} \leq n_0 \mathbb{E}_{\lambda_{\min},u} \ln\left(1+\frac{\lambda_{\min}\beta}{u}\right). \tag{55}$$

With regard to the upper bound, due to the independence of $\lambda_{\min}$ and u, (55) can be further expressed as:

$$\begin{aligned} R^{\mathrm{ZF}} &\leq n_0 \left(\mathbb{E}_{\lambda_{\min}} \left[\ln\left(\lambda_{\min}\beta\right)\right] + \sum_{t=1}^{n_0-1} \frac{1}{t} \right) \\ &+ \mathbb{E}_{\lambda_{\min}} \left[\frac{{}_2F_1\left(1,1;n_0+1;-\frac{1}{\lambda_{\min}\beta}\right)}{\lambda_{\min}\beta} \right] \end{aligned} \tag{56}$$

where ${}_2F_1$ is the hypergeometric function. Thus, an upper bound to the sum rate can be evaluated via numerical integration over the law of $\lambda_{\min}$.

We remark that an interesting line of research would be the refinement of the above upper and lower bounds for the ZF receiver. Such a refinement could be obtained, e.g., by extending the recent result in [45] to the single-branch ZF SINR.

C. Numerical Results

Here we validate the expressions of the mutual information and of the rates derived above, against numerical (i.e., Monte Carlo) simulations.

Figure 6 shows the mutual information $\mathcal{I}(\beta, n_0)$, the sum rates R^{MMSE} and R^{ZF}, and the upper and lower bounds to R^{ZF}, plotted as functions of $\mathcal{P}$, i.e., of the SNR. In this scenario, we consider a channel with one scattering cluster ($N = 2$), four transmit antennas ($n_0 = 4$), five scatterers ($n_1 = 5$), and six receive antennas ($n_2 = 6$). In the plot, the lines represent the results obtained by evaluating the expressions in (48), (51), (51), (52) and (56). Note that the lower bound in (54) is not shown, as it results to be quite loose. The markers, instead, refer to the results obtained by averaging over $M = 1000$ randomly generated samples of the matrix $\mathbf{H}$. In particular,

- square markers have been obtained by computing

$$\bar{\mathcal{I}}\left(\beta, n_0\right) = \frac{1}{M}\sum_{m=1}^{M} \ln\left|\mathbf{I} + \beta \mathbf{H}^{[m]\mathsf{H}}\mathbf{H}^{[m]}\right|$$

- circles have been obtained by computing

$$\bar{R}^{\mathrm{MMSE}} = -\frac{1}{M}\sum_{m=1}^{M}\sum_{k=1}^{n_0} \ln\left[\left(\mathbf{I} + \beta \mathbf{H}^{[m]\mathsf{H}}\mathbf{H}^{[m]}\right)^{-1}\right]_{k,k}$$

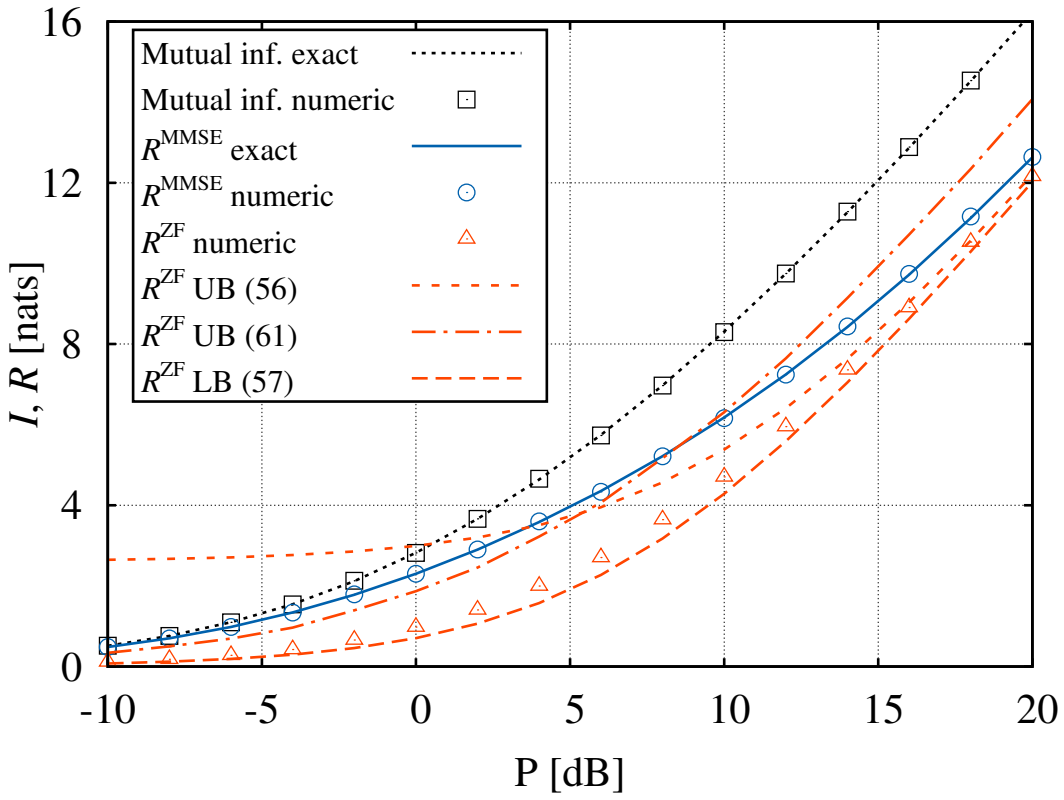

Fig. 6. Ergodic mutual information, sum rate and bounds as functions of $\mathcal{P}$, for $N = 2$, $n_0 = 4$, $n_1 = 5$, and $n_2 = 6$.

- triangles have been obtained by computing

$$\bar{R}^{\mathrm{ZF}} = -\frac{1}{M}\sum_{m=1}^{M}\sum_{k=1}^{n_0}\ln\left(1+\frac{\beta}{\left[\left(\mathbf{H}^{[m]\mathsf{H}}\mathbf{H}^{[m]}\right)^{-1}\right]_{k,k}}\right)$$

where $\mathbf{H}^{[m]}$ is the m-th realization of random matrix $\mathbf{H}$.

The figure shows a perfect match between Monte Carlo and analytical results for the MMSE case. As far as the ZF case is concerned, upper and lower bounds based on Proposition 6.1 are very tight for high SNR, while at low SNR the upper bound exhibits a floor. In this last SNR range, the upper bound (56) is to be preferred. This is in contrast with the Rayleigh fading case, for which the upper bound in [26] was generally tight over a wide range of SNR values. An intuitive explanation of this behavior is provided by the spectral density analysis in [1, Sec.

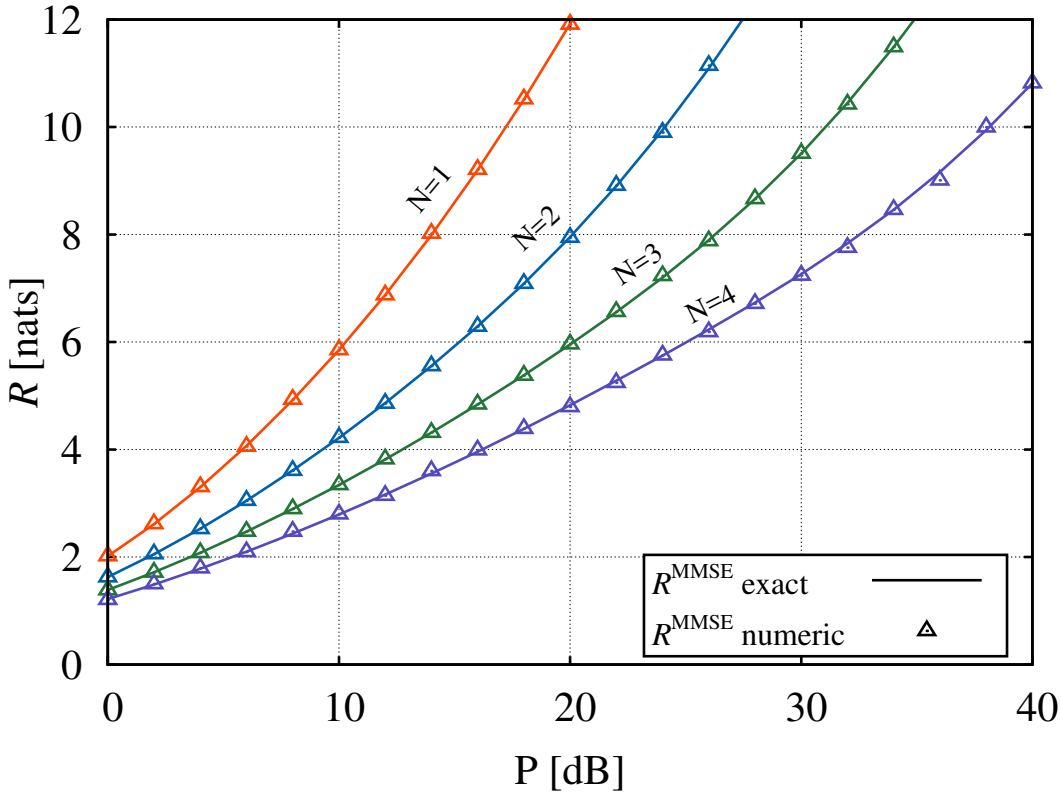

Fig. 7. Sum rates achieved by the MMSE filter plotted versus $\mathcal{P}$, for $N = 1, 2, 3, 4$, $n_i = 4$, $i = 0, \ldots, N$.

IV]. Therein, it is shown that the marginal eigenvalue density for a non-trivial (i.e., $N \geq 2$) product model exhibits a quite different behavior with respect to the Rayleigh case. Indeed, while (51) depends on the statistics of an unordered eigenvalue of $\mathbf{H}^{\mathsf{H}}\mathbf{H}$, (56) relies on the minimum eigenvalue. On the contrary, the lower bound based on $\lambda_{\min}$, and herein not depicted in any figure, is quite loose in the presence of multiple scattering.

Figures 7 and 8 show, respectively, the sum rate achieved by the MMSE filter and the corresponding gap with respect to the mutual information corresponding to the optimal case. The plots refer to the case where $N = 1, 2, 3, 4$ and $n_i = 4$, for $i = 0, \ldots, N$. For $N = 1$ the channel reduces to a classical Rayleigh MIMO without scattering clusters. As N increases, worse system performance is obtained: in particular, Figure 8 highlights that the gap between the mutual information and the MMSE rate significantly grows with N, thus suggesting that

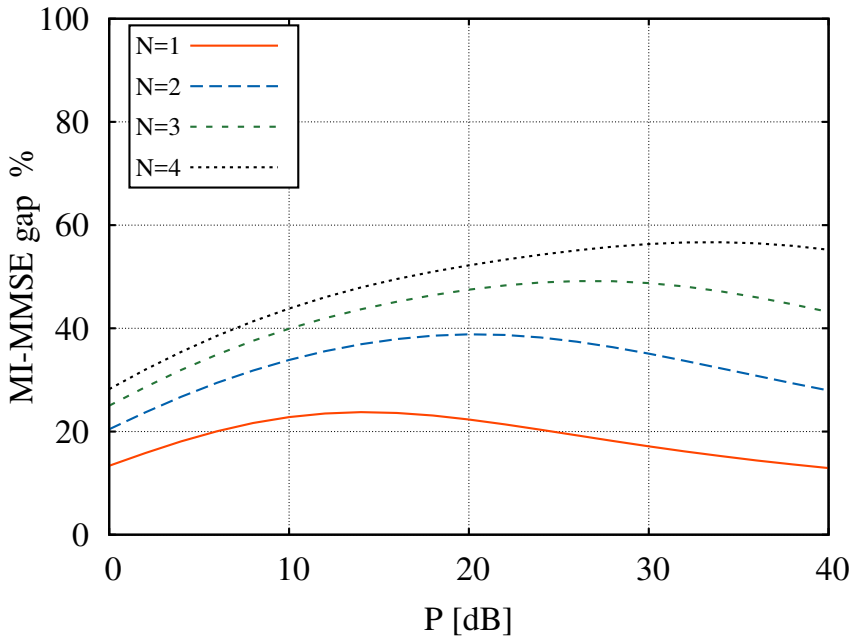

Fig. 8. Mutual information and R^{MMSE} relative difference plotted versus $\mathcal{P}$, for $N = 1, 2, 3, 4$ and $n_i = 4$, $i = 0, \ldots, N$.

linear receivers are not well-suited for multi-fold scattering.

Finally, Figure 9 depicts the ZF sum rate for different values of N and $n_i = 4$, for $i = 0, \ldots, N$. The numerical performance is shown, along with the upper bound to R^{ZF} in (56) and the lower bound in (52). Again, the rate decreases as N grows. Interestingly, the gap between the numerical curve and the upper bound decreases, while the lower bound to R^{ZF} tends to become looser.

VII. Conclusion

We investigated the performance of a MIMO link between source and destination, affected by Rayleigh fading and multiple scattering. Since the multiple-scattering channel can be represented as a finite-dimensional product of random matrices, we first analyzed the spectral properties of such product, including its generalized variance and spectral transforms. Then, under the assumption that CSI is available at the receiver only, we presented a unifying framework to evaluate in closed form the Random Coding Error Exponent, along with the cutoff rate, and the Expurgated Error Exponent. Furthermore, we analyzed the sum-rate performance when either the MMSE or the ZF receiver is adopted and independent stream decoding is used. Specifically,

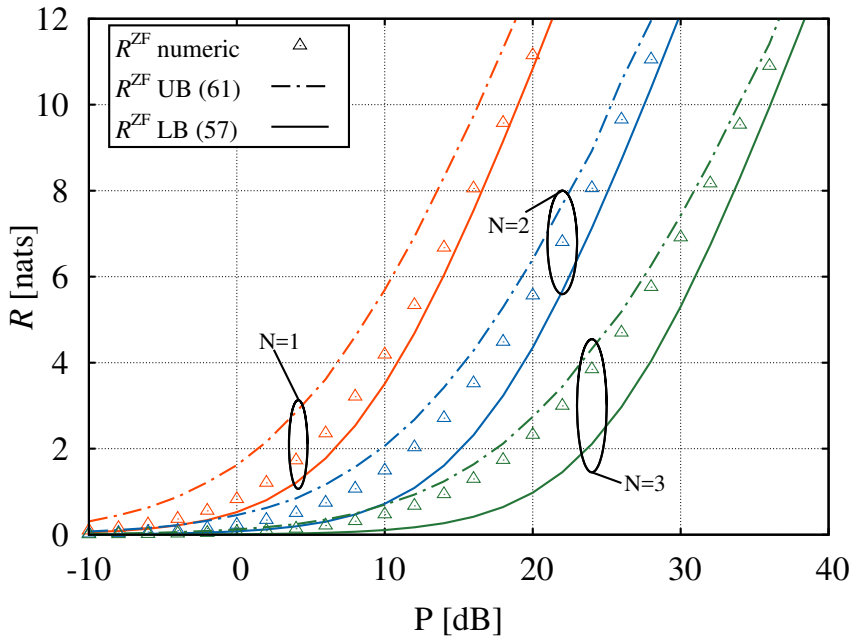

Fig. 9. Sum rates achieved by the ZF filter plotted versus $\mathcal{P}$, for $N = 1, 2, 3$ and $n_i = 4$, $i = 0, \ldots, N$.

we obtained a closed-form expression in the case of the MMSE receiver, and lower and upper bounds in the case of the ZF receiver. Importantly, our closed-form expressions hold for an arbitrary and finite number of transmit and receive antennas, and any value of SNR, while the ZF sum-rate bounds can be tailored to different, specific SNR ranges. In all cases, we validated our analysis against numerical results showing an excellent match between the two.

APPENDIX A
PROOF OF THEOREM 5.1 AND 5.2

We first prove Theorem 5.1. Under the assumption of UPA, the density of the input specified in (42) is given by

$$f_{\mathbf{X}}(\mathbf{X}) = \frac{1}{(\pi p)^{n_c n_0}} \exp\left(-\frac{\|\mathbf{X}\|^2}{p}\right).$$

The conditional law $f(\mathbf{Y}|\mathbf{X}, \mathbf{H})$ appearing in (37) is Gaussian non-central matrix-variate and can be written as

$$f(\mathbf{Y}|\mathbf{X}, \mathbf{H}) = \exp\left(-\|\mathbf{Y} - \sqrt{\alpha}\mathbf{H}\mathbf{X}\|^2\right) \pi^{-n_N n_c}. \quad (57)$$

Let $t(\mathbf{Y},\mathbf{H})$ be the average over $\mathbf{X}$ appearing in (37). Then

$$\begin{aligned} t(\mathbf{Y},\mathbf{H}) &= \mathbb{E}_{\mathbf{X}}\left[f(\mathbf{Y}|\mathbf{X},\mathbf{H})^{\frac{1}{1+\rho}}\mathrm{e}^{r(\|\mathbf{X}\|^2-n_c\mathcal{P})}\right] \\ &= \int_{\mathbb{C}^{n_0\times n_c}} f_{\mathbf{X}}(\mathbf{X}) f(\mathbf{Y}|\mathbf{X},\mathbf{H})^{\frac{1}{1+\rho}}\mathrm{e}^{r(\|\mathbf{X}\|^2-n_c\mathcal{P})}\,\mathrm{d}\mathbf{X}\,. \end{aligned}$$

By substituting in the above equation the expressions for $f_{\mathbf{X}}(\mathbf{X})$ and $f(\mathbf{Y}|\mathbf{X},\mathbf{H})$, we obtain

$$\begin{aligned} t(\mathbf{Y},\mathbf{H}) &= c\int \mathrm{e}^{\mathsf{Tr}\left\{-\mathbf{L}\mathbf{X}\mathbf{X}^{\mathsf{H}}+\frac{\sqrt{\alpha}}{1+\rho}\left(\mathbf{H}^{\mathsf{H}}\mathbf{Y}\mathbf{X}^{\mathsf{H}}+\mathbf{X}\mathbf{Y}^{\mathsf{H}}\mathbf{H}\right)\right\}}\,\mathrm{d}\mathbf{X} \\ &\overset{(a)}{=} \frac{c\pi^{n_c n_0}}{|\mathbf{L}|^{n_c}}\mathrm{e}^{\mathsf{Tr}\left\{\frac{\alpha}{(1+\rho)^2}\mathbf{H}\mathbf{L}^{-1}\mathbf{H}^{\mathsf{H}}\mathbf{Y}\mathbf{Y}^{\mathsf{H}}\right\}} \\ &= \frac{\mathrm{e}^{-rn_c\mathcal{P}}\mathrm{e}^{\mathsf{Tr}\left\{\left(\frac{\alpha}{(1+\rho)^2}\mathbf{H}\mathbf{L}^{-1}\mathbf{H}^{\mathsf{H}}-\frac{1}{1+\rho}\mathbf{I}\right)\mathbf{Y}\mathbf{Y}^{\mathsf{H}}\right\}}}{\pi^{\frac{n_N n_c}{1+\rho}}|p\mathbf{L}|^{n_c}} \end{aligned} \tag{58}$$

where $c=\mathrm{e}^{-rn_c\mathcal{P}-\frac{\|\mathbf{Y}\|^2}{1+\rho}}/(p^{n_c n_0}\pi^{n_c n_0+\frac{n_N n_c}{1+\rho}})$ and

$$\mathbf{L}=\left(\frac{n_0-r\mathcal{P}}{\mathcal{P}}\right)\mathbf{I}+\frac{\alpha}{1+\rho}\mathbf{H}^{\mathsf{H}}\mathbf{H}\,, \tag{59}$$

and where the equality (a) relies on the result in [46, Appendix B] [9]. We now compute the integral with respect to $\mathbf{Y}$ appearing in (37). We have

$$\begin{aligned} s(\mathbf{H}) &= \int_{\mathbb{C}^{n_N\times n_c}} t(\mathbf{Y},\mathbf{H})^{1+\rho}\,\mathrm{d}\mathbf{Y} \\ &= \frac{\mathrm{e}^{-rn_c\mathcal{P}(1+\rho)}}{|p\mathbf{L}|^{n_c(1+\rho)}}\int_{\mathbb{C}^{n_N\times n_c}}\frac{\mathrm{e}^{-\mathsf{Tr}\{(\mathbf{I}-\frac{\alpha}{1+\rho}\mathbf{H}\mathbf{L}^{-1}\mathbf{H}^{\mathsf{H}})\mathbf{Y}\mathbf{Y}^{\mathsf{H}}\}}}{\pi^{n_N n_c}}\,\mathrm{d}\mathbf{Y}\,. \end{aligned}$$

The above integral can be solved by using the property

$$\int_{\mathbb{C}^{n_N\times n_c}}\frac{\mathrm{e}^{-\mathsf{Tr}\{\mathbf{M}^{-1}\mathbf{Y}\mathbf{Y}^{\mathsf{H}}\}}}{\pi^{n_N n_c}|\mathbf{M}|^{n_c}}\,\mathrm{d}\mathbf{Y}=1$$

which holds for any invertible square matrix $\mathbf{M}$. Then we get

$$\begin{aligned} s(\mathbf{H}) &= \frac{\mathrm{e}^{-rn_c\mathcal{P}(1+\rho)}}{|p\mathbf{L}|^{n_c(1+\rho)}}\left|\mathbf{I}-\frac{\alpha}{1+\rho}\mathbf{H}\mathbf{L}^{-1}\mathbf{H}^{\mathsf{H}}\right|^{-n_c} \\ &= \frac{\mathrm{e}^{-rn_c\mathcal{P}(1+\rho)}}{|p\mathbf{L}|^{n_c(1+\rho)}}\left|\frac{p}{1-pr}\mathbf{L}\right|^{n_c} \\ &= \frac{\mathrm{e}^{-rn_c\mathcal{P}(1+\rho)}}{|p\mathbf{L}|^{n_c\rho}(1-pr)^{n_c n_0}}. \end{aligned} \tag{60}$$

[9] Notice that the referred formula assumes a positive definite $\mathbf{L}$. Positive definiteness of (59) is indeed ensured by enforcing the constraint $0\le n_0-r\mathcal{P}\le n_0$, as customary in the literature (see e.g., [17, Eq.(16)]).

We observe that $s(\mathbf{H})$ depends on $\mathbf{H}$ only through its non-zero squared singular values, i.e., the eigenvalues $\mathbf{\Lambda} = \mathrm{diag}(\lambda_1, \ldots, \lambda_{n_0})$ of $\mathbf{H}\mathbf{H}^{\mathsf{H}}$, appearing in $|\mathbf{L}|$. Indeed, by using the definition of $\mathbf{L}$ given in (59), we have

$$|p\mathbf{L}| = (1-pr)^{n_0} \left| \mathbf{I} + \frac{\alpha p}{(1+\rho)(1-pr)} \mathbf{\Lambda} \right| .$$

Thus, we can write:

$$s(\mathbf{H}) = \tilde{s}(\mathbf{\Lambda}) = \frac{\mathrm{e}^{-rn_c\mathcal{P}(1+\rho)}}{(1-pr)^{n_c n_0(1+\rho)}} \left| \mathbf{I} + \frac{\alpha p}{(1+\rho)(1-pr)} \mathbf{\Lambda} \right|^{-n_c\rho} .$$

As a consequence, the outer integral in the expression of the error exponent (i.e., the integration over $\mathbf{H}$) can be computed as

$$\mathcal{E} = \mathbb{E}_{\mathbf{H}}[s(\mathbf{H})] = \int_{\mathbb{C}^{n_N \times n_0}} f_{\mathbf{H}}(\mathbf{H}) s(\mathbf{H}) \, \mathrm{d}\mathbf{H} = \int_{(\mathbb{R}+)^{n_0}} f_{\mathbf{\Lambda}}(\mathbf{\Lambda}) \tilde{s}(\mathbf{\Lambda}) \, \mathrm{d}\mathbf{\Lambda} \tag{61}$$

where in the last equality we first applied the change of integration variable $\mathbf{H}^{\mathsf{H}}\mathbf{H} = \mathbf{U}\mathbf{\Lambda}\mathbf{U}^{\mathsf{H}}$ (with $\mathbf{U}$ being a unitary matrix) and then the result in [30, eq. (93)]. By substituting in (61) the expression for $\tilde{s}(\mathbf{\Lambda})$, we obtain (43). Notice that, in the presence of a generic input-covariance $\mathbf{Q}$, repeatedly applying [46, Appendix B] would have led to the very same expression as in [17, (15)].

Theorem 5.2 can be proved in a similar way. Specifically, the integral in (41) is evaluated by using the expression for $f(\mathbf{Y}|\mathbf{X}, \mathbf{H})$ in (57) and by resorting to [46, Appendix B], i.e.,

$$\begin{aligned} w(\mathbf{X}, \mathbf{X}', \mathbf{H}) &= \frac{\mathrm{e}^{-\alpha\|\mathbf{H}\mathbf{X}\|^2/2 - \alpha\|\mathbf{H}\mathbf{X}'\|^2/2}}{\pi^{n_N n_c}} \cdot \\ &\quad \int_{\mathbb{C}^{n_N \times n_c}} \mathrm{e}^{-\mathsf{Tr}\{\frac{2\mathbf{Y}\mathbf{Y}^{\mathsf{H}} - \sqrt{\alpha}\mathbf{Y}(\mathbf{X}+\mathbf{X}')^{\mathsf{H}}\mathbf{H}^{\mathsf{H}} + \sqrt{\alpha}\mathbf{H}(\mathbf{X}+\mathbf{X}')\mathbf{Y}^{\mathsf{H}}}{2}\}} \, \mathrm{d}\mathbf{Y} \\ &= \mathrm{e}^{-\alpha\|\mathbf{H}\mathbf{X}\|^2/2 - \alpha\|\mathbf{H}\mathbf{X}'\|^2/2 + \alpha\|\mathbf{H}(\mathbf{X}+\mathbf{X}')\|^2/4} \\ &= \mathrm{e}^{-\alpha\|\mathbf{H}(\mathbf{X}-\mathbf{X}')\|^2/4} . \end{aligned} \tag{62}$$

As far as the computation of (40) is concerned, we first average with respect to $\mathbf{X}'$. This average too admits closed-form expression by virtue of [46, Appendix B]. Indeed, we have

$$\begin{aligned} v(\mathbf{X}, \mathbf{H}) &= \mathbb{E}_{\mathbf{X}'} \left[\mathrm{e}^{r\|\mathbf{X}'\|^2} w(\mathbf{X}, \mathbf{X}', \mathbf{H})^{\frac{1}{\rho}} \right] \\ &= \int_{\mathbb{C}^{n_0 \times n_c}} f_{\mathbf{X}'}(\mathbf{X}') \mathrm{e}^{r\|\mathbf{X}'\|^2} \mathrm{e}^{-\alpha\|\mathbf{H}(\mathbf{X}-\mathbf{X}')\|^2/4\rho} \, \mathrm{d}\mathbf{X}' \\ &= (\pi p)^{-n_0 n_c} \mathrm{e}^{-\alpha\|\mathbf{H}\mathbf{X}\|^2/4\rho} \\ &\quad \int_{\mathbb{C}^{n_0 \times n_c}} \mathrm{e}^{-\mathsf{Tr}\left\{\mathbf{X}'\mathbf{X}'^{\mathsf{H}}\mathbf{L}_e - \frac{\alpha\mathbf{H}^{\mathsf{H}}\mathbf{H}\mathbf{X}\mathbf{X}'^{\mathsf{H}}}{4\rho} - \frac{\alpha\mathbf{X}^{\mathsf{H}}\mathbf{H}^{\mathsf{H}}\mathbf{H}\mathbf{X}'}{4\rho}\right\}} \, \mathrm{d}\mathbf{X}' \\ &= |p\mathbf{L}_e|^{-n_c} \mathrm{e}^{-\alpha\|\mathbf{H}\mathbf{X}\|^2/4\rho} \mathrm{e}^{\mathsf{Tr}\{\mathbf{W}\mathbf{X}\mathbf{X}^{\mathsf{H}}\}} \end{aligned} \tag{63}$$

where

$$\mathbf{L}_e = \left(\frac{n_0 - r\mathcal{P}}{\mathcal{P}}\right)\mathbf{I} + \frac{\alpha}{4\rho}\mathbf{H}^{\mathsf{H}}\mathbf{H}$$

and

$$\mathbf{W} = \frac{\alpha^2}{16\rho^2}\mathbf{H}^{\mathsf{H}}\mathbf{H}\mathbf{L}_e^{-1}\mathbf{H}^{\mathsf{H}}\mathbf{H}\,.$$

We now average with respect to $\mathbf{X}$ and obtain

$$\begin{aligned} s_e(\mathbf{H}) &= \mathbb{E}_{\mathbf{X}}\left[\mathrm{e}^{r\|\mathbf{X}\|^2} v(\mathbf{X},\mathbf{H})\right] \\ &= \int_{\mathbb{C}^{n_0\times n_c}} \frac{\mathrm{e}^{-\mathsf{Tr}\left\{(\mathbf{L}_e-\mathbf{W})\mathbf{X}\mathbf{X}^{\mathsf{H}}\right\}}}{|\pi p^2 \mathbf{L}_e|^{n_c}}\,\mathrm{d}\mathbf{X} \\ &= |p^2\mathbf{L}_e(\mathbf{L}_e-\mathbf{W})|^{-n_c}\,. \end{aligned} \tag{64}$$

Then, by substituting the expressions for $\mathbf{L}_e$ and $\mathbf{W}$, we get

$$s_e(\mathbf{H}) = (1-pr)^{-2n_c n_0}\left|\mathbf{I} + \frac{\alpha p}{2\rho(1-pr)}\mathbf{\Lambda}\right|^{-n_c}. \tag{65}$$

Note that also $s_e(\mathbf{H})$ depends on the eigenvalues $\mathbf{\Lambda}$ of $\mathbf{H}^{\mathsf{H}}\mathbf{H}$. Under the assumption that the density of $\mathbf{H}$ depends only on $\mathbf{H}^{\mathsf{H}}\mathbf{H}$, the integral in (40) provides the result reported in (45).

APPENDIX B
PROOF OF PROPOSITION 5.1 AND 5.2

We start by proving Proposition 5.1. Following Theorems 5.1 and 5.2, the only quantity that has to be provided to perform error exponents evaluation is the joint law of the non-zero ordered eigenvalues of $\mathbf{H}\mathbf{H}^{\mathsf{H}}$. If $\mathbf{H}$ is given by (3), where each factor is an i.i.d. Gaussian matrix, then [32]

$$f_{\mathbf{\Lambda}}(\mathbf{\Lambda}) = \frac{1}{n_0!|\mathbf{A}_0|}V(\mathbf{\Lambda})|\mathbf{G}(\mathbf{\Lambda})|\,. \tag{66}$$

$\mathbf{G}$ is an $n_0 \times n_0$ matrix such that

$$[\mathbf{G}(\mathbf{\Lambda})]_{i,j} = G_{0,N}^{N,0}\left(\begin{array}{c} - \\ \nu_N,\ldots,\nu_2,\nu_1+i-1 \end{array}\middle|\,\lambda_j\right),$$

for $i,j = 1,\ldots,n_0$. Then the matrix integral $\mathcal{E}$ boils down to

$$\mathcal{E} = \frac{k}{n_0!|\mathbf{A}_0|}\int_{(\mathbb{R}^+)^{n_0}} V(\mathbf{\Lambda})|\mathbf{G}(\mathbf{\Lambda})|\left|\mathbf{I} + \frac{\alpha p}{(1+\rho)(1-pr)}\mathbf{\Lambda}\right|^{-n_c\rho}\mathrm{d}\mathbf{\Lambda}. \tag{67}$$

As far as the EEE evaluation is concerned,

$$\mathcal{E}_e = \frac{k_e}{n_0!|\mathbf{A}_0|}\int_{(\mathbb{R}^+)^{n_0}} V(\mathbf{\Lambda})|\mathbf{G}(\mathbf{\Lambda})|\left|\mathbf{I} + \frac{\alpha p}{2\rho(1-pr)}\mathbf{\Lambda}\right|^{-n_c\rho}\mathrm{d}\mathbf{\Lambda} \tag{68}$$

is to be computed. Both (67) and (68) can be expressed in closed form according to [38, Corollary I], so that

$$\mathcal{E} = \frac{k}{|\mathbf{A}_0|}\left|\mathbf{Z}\left(\frac{(1+\rho)(1-pr)}{\alpha p}\right)\right|, \tag{69}$$

with the entries of $\mathbf{Z}$ given by

$$[\mathbf{Z}(x)]_{i,j} = \int_0^{+\infty} \frac{G_{0,N}^{N,0}\left(\begin{array}{c} - \\ \nu_N,\ldots,\nu_2,\nu_1+i-1 \end{array}\middle|\lambda\right)}{\lambda^{1-j}\,(1+\lambda/x)^{n_c\rho}}\,\mathrm{d}\lambda\,.$$

The above integral can be solved by using the result in [29, 7.811.5] yielding (45). Similarly,

$$\mathcal{E}_e = \frac{k_e}{|\mathbf{A}_0|}\left|\mathbf{Z}\left(\frac{2\rho(1-pr)}{\alpha p}\right)\right|.$$

APPENDIX C
PROOF OF (10)

We first observe that the i,j-th element of $\mathbf{A}_0$ can be written as

$$\begin{aligned}[\mathbf{A}_0]_{i,j} &= \Gamma(\nu_1+i+j-1)\prod_{\ell=2}^{N}\Gamma(\nu_\ell+j)\\ &= [\mathbf{B}]_{i,j}[\mathbf{C}]_{j,j}\end{aligned} \tag{70}$$

where $[\mathbf{B}]_{i,j} = \Gamma(\nu_1+i+j-1)$ and $\mathbf{C}$ is diagonal with entries $[\mathbf{C}]_{i,i} = \prod_{\ell=2}^{N}\Gamma(\nu_\ell+i)$. Then $\mathbf{A}_0 = \mathbf{BC}$ and $|\mathbf{A}_0| = |\mathbf{B}||\mathbf{C}|$. Note that

$$|\mathbf{C}| = \prod_{i=1}^{n_0}[\mathbf{C}]_{i,i} = \prod_{i=1}^{n_0}\prod_{\ell=2}^{N}\Gamma(\nu_\ell+i)\,.$$

As far as $|\mathbf{B}|$ is concerned, we have

$$\begin{aligned}|\mathbf{B}| &= \left|\{\Gamma(\nu_1+i+j-1)\}\right|_{i,j=1,\ldots,n_0}\\ &= \left|\{\Gamma(\nu_1+i+j+1)\}\right|_{i,j=0,\ldots,n_0-1}\\ &= \left|\{\Gamma(z_j+i)\}\right|_{i,j=0,\ldots,n_0-1}\end{aligned} \tag{71}$$

where $z_j = \nu_1 + j + 1$. We now exploit the result in [47, Eq. (4.1)] and obtain:

$$\begin{aligned}
|\mathbf{B}| &= \left|\{\Gamma(z_j + i)\}\right|_{i,j=0,\ldots,n_0-1} \\
&= \left[\prod_{j=0}^{n_0-1} \Gamma(z_j)\right] V(\mathbf{E}) \\
&= \prod_{j=0}^{n_0-1} \Gamma(z_j) \prod_{j=0}^{n_0-1} \Gamma(j+1) \\
&= \prod_{j=0}^{n_0-1} \Gamma(\nu_1 + j + 1) \prod_{j=0}^{n_0-1} \Gamma(j+1) \\
&= \prod_{j=1}^{n_0} \Gamma(\nu_1 + j) \prod_{j=1}^{n_0} \Gamma(j) \\
&= \prod_{i=1}^{n_0} \prod_{\ell=0}^{1} \Gamma(\nu_\ell + i)
\end{aligned} \tag{72}$$

where $\mathbf{E} = \mathrm{diag}(z_0, \ldots, z_{n_0-1})$ and we applied [47, Eq. (B.5)]. With regard to the last line, we recall that $\nu_0 = 0$ by definition.

In conclusion,

$$\begin{aligned}
|\mathbf{A}_0| &= \left[\prod_{i=1}^{n_0} \prod_{\ell=0}^{1} \Gamma(\nu_\ell + i)\right] \left[\prod_{i=1}^{n_0} \prod_{\ell=2}^{N} \Gamma(\nu_\ell + i)\right] \\
&= \prod_{i=1}^{n_0} \prod_{\ell=0}^{N} \Gamma(\nu_\ell + i)\,.
\end{aligned} \tag{73}$$

which corresponds to $\mathcal{Z}/n_0!$.

REFERENCES

[1] G. Akemann, J. Ipsen, M. Kieburg, "Products of rectangular random matrices: singular values and progressive scattering," *APS Physical Review E*, Vol. 88, No. 3, 2013.

[2] D. Gesbert, H. Bölcskei, D. A. Gore, A. J. Paulraj,"Outdoor MIMO wireless channels: Models and performance prediction," *IEEE Transactions on Communications*, Vol. 50, No. 12, pp. 1926–1934, Dec. 2002.

[3] R. Muller, "On the asymptotic eigenvalue distribution of concatenated vector-valued fading channels," *IEEE Transactions on Information Theory*, Vol. 48, No. 7, pp. 2086–2091, July 2002.

[4] P. Almers, F. Tufvesson, A. Molisch, "Keyhole effects in MIMO wireless channels-measurements and theory," *IEEE Globecom*, 2003.

[5] G. Levin, S. Loyka, "From multi-keyholes to measure of correlation and power imbalance in MIMO channels: Outage capacity analysis," *IEEE Transactions on Information Theory*, Vol. 57, No. 6, pp. 3515–3529, June 2011.

[6] H. Shin, J. H. Lee, "Capacity of multiple-antenna fading channels: Spatial fading correlation, double scattering, and keyhole," *IEEE Transactions on Information Theory*, Vol. 49, No. 10, pp. 2636–2646, Oct. 2003.

[7] L. Wei, Z. Zheng, O. Tirkkonen, J. Hamalainen, "On the ergodic mutual information of multiple cluster scattering MIMO channels," *IEEE Communications Letters,* Vol. 17, No. 9, pp. 1700–1703, 2013.

[8] M. Haenggi, "5G: The quest for cell-less cellular networks," *Keynote talk*, *IEEE CTW*, May 2014.

[9] L. Wei, "Ergodic capacity of spatially correlated multi-cluster scattering MIMO channels," *IEEE ISIT,* Hong Kong, June 2015.

[10] H. Shin, M. Z. Win, "MIMO diversity in the presence of double scattering," *IEEE Transactions on Information Theory* Vol. 54, No. 7, pp. 2976–2996, July 2008.

[11] Z. Zheng, L. Wei, R. Speicher, R. Muller, J. Hamalainen, J. Corander, "Asymptotic analysis of Rayleigh product channels: A free probability approach," *IEEE Transactions on Information Theory*, Vol. 63, No. 3, pp. 1731–1745, Mar. 2017.

[12] C. Zhong, T. Ratnarajah, Z. Zhang, K.-K. Wong, M. Sellathurai, "Performance of Rayleigh product MIMO channels with linear receivers," *IEEE Transactions on Wireless Communications*, Vol. 13, No. 4, pp. 2270–2281, Apr. 2014.

[13] S. Yeh, O. Lévêque, "Asymptotic capacity of multi-level amplify-and-forward relay networks," *IEEE ISIT 2007*, Nice, France, June 2007.

[14] N. Fawaz, K. Zarifi, M. Debbah, D. Gesbert, "Asymptotic capacity and optimal precoding of multi-hop relaying systems," *IEEE Transactions on Information Theory,* Vol. 57, No. 4, pp. 2050–2069, Apr. 2011.

[15] L. Wei, Z. Zheng, J. Corander, G. Taricco, "On the outage capacity of orthogonal space-time block codes over multi-cluster scattering MIMO channels," *IEEE Transactions on Communications*, Vol. 63, No. 5, pp. 1700–1711, Dec. 2015.

[16] R. G. Gallager, *Information Theory and Reliable Communication,* New York, Wiley, 1968.

[17] H. Shin, M. Z. Win, "Gallager's exponent for MIMO channels: A reliability-rate tradeoff,"*IEEE Transactions on Communications*, Vol. 57, No. 4, pp. 972–985, Apr. 2009.

[18] J. Xue, T. Ratnarajah, C. Zhong, C.-K. Wen, "Reliability analysis for large MIMO systems," *IEEE Wireless Communications Letters*, Vol. 3, No. 6, pp. 553–556, Dec. 2014.

[19] J. Xue, M. Z. I. Sarkar, T. Ratnarajah, C. Zhong: "Error exponents for Rayleigh fading product MIMO channels," *IEEE ISIT,* Cambridge MA, USA, July 2012.

[20] J. Xue, T. Ratnarajah, C. Zhong, "Error exponents for multi-keyhole MIMO channels," *Problems of Information Transmission*, Vol. 51, No. 1, pp. 1–19, Jan. 2015.

[21] J. Zhang, M. Matthaiou, G. Karagiannidis, H. Wang, Z. Tan, "Gallager's exponent analysis of STBC MIMO systems over η-μ and κ-μ fading channels," *IEEE Transactions on Communications*, Vol. 61, No. 3, pp. 1028–1039, 2013.

[22] I. E. Telatar, "Capacity of multi-antenna Gaussian channels," *AT&T Bell Laboratories Technical Report,* BL0112170-950615-07TM, June 1995.

[23] I. Abou-Faycal, B. Hochwald, "Coding requirements for multiple-antenna channels with unknown Rayleigh fading," *Bell Labs Tech. Mem.*, 1999.

[24] D. E. Simmons, J. P. Coon, N. Warsi, "Capacity and power scaling laws for finite antenna MIMO amplify-and-forward relay networks," *IEEE Transactions on Information Theory,* Vol. 62, No. 4, pp. 1993–2008, Apr. 2016.

[25] M. R. McKay, I. B. Collings, A. M. Tulino, "Achievable sum rate of MIMO MMSE receivers: A general analytic framework," *IEEE Transactions on Information Theory,* Vol. 56, No. 1, pp. 396–410, Jan. 2010.

[26] M. Matthaiou, C. Zhong, T. Ratnarajah, "Novel generic bounds on the sum rate of MIMO ZF receivers," *IEEE Transactions on Signal Processing*, Vol. 59, No. 9, pp. 4341–4353, Sep. 2011.

[27] M. Matthaiou, C. Zhong, M. R. McKay, T. Ratnarajah, "Sum rate analysis of ZF receivers in distributed MIMO systems," *IEEE Journal on Selected Areas in Communications,* Vol. 31, No. 2, pp. 180–191, Feb. 2013.

[28] Y. Jiang, M. K. Varanasi, J. Li, "Performance analysis of ZF and MMSE equalizers for MIMO systems: An in-Depth study of the high SNR regime," *IEEE Transactions on Information Theory*, Vol. 57, No. 4, pp. 6788–6805, Apr. 2011.

[29] I. S. Gradshteyn, I. M. Ryzhik, *Table of integrals, series, and products*, Academic Press, New York, 1980.

[30] A. T. James, "Distribution of matrix variates and latent roots derived from normal samples," *The Annals of Mathematical Statistics,* Vol. 35, No. 2, pp. 474–501, June 1964.

[31] A. Tulino, S. Verdú, "Random matrices and wireless communications," *Foundations and Trends in Communications and Information Theory,* Vol. 1, No. 1, July 2004.

[32] A. Kuijlaars, D. Stivigny, "Singular values of products of random matrices and polynomial ensembles," *Random Matrices: Theory and Application,* Vol. 3, No. 3, pp. 1–22, 2014.

[33] G. Alfano, A. Tulino, A. Lozano, S. Verdú, "Eigenvalue statistics of finite-dimensional random matrices for MIMO wireless communications," *IEEE International Conference on Communications (ICC)*, Istanbul, Turkey, June 2006.

[34] J. Salo, H. M. El-Sallabi, P. Vainikainen, "Distribution of the Product of Independent Rayleigh Random Variables," *IEEE Transactions in Antennas and Propagation,* Vol. 54, No. 2, pp. 639–643, Feb. 2006.

[35] M. Chiani, M. Z. Win, A. Zanella, "On the marginal distribution of the eigenvalues of Wishart matrices," *IEEE Transactions on Wireless Communications,* Vol. 57, No. 4, pp. 1050–1060, Apr. 2009.

[36] M. Kang, M.-S. Alouini, "Largest eigenvalue of complex Wishart matrices and performance analysis of MIMO MRC systems," *IEEE Journal on Selected Areas in Commununications*, Vol. 21, No. 3, pp. 418–426, Apr. 2003.

[37] R. Bellmann, Introduction to Matrix Analysis *SIAM*, 1987.

[38] M. Chiani, M. Z. Win, A. Zanella, "On the capacity of spatially correlated MIMO Rayleigh-fading channels," *IEEE Transactions on Information Theory,* Vol. 49, No. 10, pp. 2363–2371, Oct. 2003.

[39] G. Alfano, C-F. Chiasserini, A. Nordio, S. Zhou, "A unifying analysis of error exponents for MIMO channels with application to multiple-scattering," *Special Session on Advancements in Wireless Communications, IEEE ISWCS*, Bruxelles, Aug. 2015.

[40] G. Alfano, C. F. Chiasserini, A. Nordio, "Achievable sum rate of linear MIMO receivers with multiple Rayleigh scattering," *20th International ITG Workshop on Smart Antennas (WSA)*, Munich, Germany, 2016.

[41] S. Verdú, *Multiuser Detection*, Cambridge University Press, 2011.

[42] H. Gao, P. J. Smith, M. V. Clark, "Theoretical reliability of MMSE linear diversity combining in Rayleigh-fading additive interference channels," *IEEE Transactions on Communications,* Vol. 46, No. 5, pp. 666–672, May 2003.

[43] R. A. Horn, C. R. Johnson, *Matrix Analysis,* 4th ed., Cambridge University Press, 1990.

[44] R. Narasimhan, "Spatial multiplexing with transmit antenna and constellation selection for correlated MIMO fading channels," *IEEE Transactions on Signal Processing*, Vol. 51, No. 11, pp. 2829-2838, Nov. 2003.

[45] J. Yuan, M. Matthaiou, S. Jin, F. Gao, "Tightness of Jensens bounds and applications to MIMO communications," *IEEE Transactions on Communications*, Vol. 65, No. 2, pp. 579–593, Feb. 2017.

[46] G. Taricco, "Asymptotic mutual information statistics of separately correlated Rician fading MIMO channels," *IEEE Transactions on Information Theory*, Vol. 54, No. 8, pp. 3490–3504, Aug. 2008.

[47] J.-M. Normand, "Calculation of some determinants using the s-shifted factorial," *Journal of Physics A: Mathematical and General,* Vol. 37, No. 22, pp. 5737–5762, 2004.